

Role of aldehyde chemistry and NO_x concentrations in secondary organic aerosol formation

A. W. H. Chan¹, M. N. Chan², J. D. Surratt^{1,*}, P. S. Chhabra¹, C. L. Loza¹, J. D. Crouse¹, L. D. Yee², R. C. Flagan^{1,2}, P. O. Wennberg^{2,3}, and J. H. Seinfeld^{1,2}

¹Division of Chemistry and Chemical Engineering, California Institute of Technology, Pasadena, CA, USA

²Division of Engineering and Applied Science, California Institute of Technology, Pasadena, CA, USA

³Division of Geological and Planetary Sciences, California Institute of Technology, Pasadena, CA, USA

* now at: Department of Environmental Sciences and Engineering, The University of North Carolina at Chapel Hill, Chapel Hill, NC, USA

Received: 7 April 2010 – Published in Atmos. Chem. Phys. Discuss.: 19 April 2010

Revised: 13 July 2010 – Accepted: 16 July 2010 – Published: 4 August 2010

Abstract. Aldehydes are an important class of products from atmospheric oxidation of hydrocarbons. Isoprene (2-methyl-1,3-butadiene), the most abundantly emitted atmospheric non-methane hydrocarbon, produces a significant amount of secondary organic aerosol (SOA) via methacrolein (a C₄-unsaturated aldehyde) under urban high-NO_x conditions. Previously, we have identified peroxy methacryloyl nitrate (MPAN) as the important intermediate to isoprene and methacrolein SOA in this NO_x regime. Here we show that as a result of this chemistry, NO₂ enhances SOA formation from methacrolein and two other α,β -unsaturated aldehydes, specifically acrolein and crotonaldehyde, a NO_x effect on SOA formation previously unrecognized. Oligoesters of dihydroxycarboxylic acids and hydroxynitrooxycarboxylic acids are observed to increase with increasing NO₂/NO ratio, and previous characterizations are confirmed by both online and offline high-resolution mass spectrometry techniques. Molecular structure also determines the amount of SOA formation, as the SOA mass yields are the highest for aldehydes that are α,β -unsaturated and contain an additional methyl group on the α -carbon. Aerosol formation from 2-methyl-3-buten-2-ol (MBO232) is insignificant, even under high-NO₂ conditions, as PAN (peroxy acyl nitrate, RC(O)OONO₂) formation is structurally unfavorable. At atmospherically relevant NO₂/NO ratios (3–8), the SOA yields from isoprene high-NO_x photooxidation are 3 times greater than previously measured at lower NO₂/NO ratios. At sufficiently high NO₂ concentrations, in systems of α,β -

unsaturated aldehydes, SOA formation from subsequent oxidation of products from acyl peroxy radicals+NO₂ can exceed that from RO₂+HO₂ reactions under the same inorganic seed conditions, making RO₂+NO₂ an important channel for SOA formation.

1 Introduction

Organic matter is ubiquitous in atmospheric aerosols and accounts for a major fraction of particulate matter mass (Zhang et al., 2007a). Most particulate organic matter (POM) is secondary in origin, comprising condensable oxidation products of gas-phase volatile organic compounds (VOCs) (Hallquist et al., 2009). Despite the importance of secondary organic aerosol (SOA), its sources and formation processes are not fully understood. Global modeling studies predict that oxidation of biogenic hydrocarbons dominates the global SOA burden owing to high emissions and efficient SOA production (Chung and Seinfeld, 2002; Kanakidou et al., 2005; Henze and Seinfeld, 2006). This is supported by observations of high levels of modern (hence biogenic) carbon in ambient particulate organic matter, even in urban centers such as Nashville, TN, Tampa, FL and Atlanta, GA (Lewis et al., 2004; Lewis and Stiles, 2006; Weber et al., 2007). However, field observations have repeatedly shown that SOA formation is highly correlated with anthropogenic tracers, such as CO and acetylene (de Gouw et al., 2005, 2008).

A considerable body of laboratory chamber studies have investigated the dependence of SOA yields (mass of SOA formed per mass of hydrocarbon reacted) on NO_x level, which can vary greatly between urban and remote

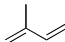
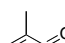
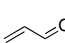
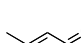
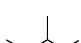
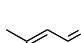


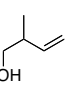
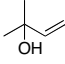


Correspondence to: J. H. Seinfeld
(seinfeld@caltech.edu)

areas. For photooxidation and ozonolysis of monoterpenes (Hatakeyama et al., 1991; Ng et al., 2007a; Zhang et al., 2007b; Presto et al., 2005), monocyclic (Song et al., 2005; Hurley et al., 2001; Ng et al., 2007b) and polycyclic aromatic compounds (Chan et al., 2009b), SOA yields are larger under low-NO_x conditions; for sesquiterpenes, the reverse is true (Ng et al., 2007a). SOA formation from photooxidation of isoprene exhibits especially complex behavior depending on the NO_x level (Kroll et al., 2006). The effect of NO_x level on SOA formation has generally been attributed to the relative reaction rates of peroxy radicals (RO₂) with NO and HO₂ and the difference in volatilities of the products from the respective pathways (Kroll and Seinfeld, 2008). Under high-NO_x conditions, RO₂+NO dominates and leads to formation of fragmentation products or organic nitrates, which are generally volatile (Presto et al., 2005). On the contrary, the RO₂+HO₂ pathway, which is competitive only when [NO] << 1 ppb, produces less volatile hydroxyhydroperoxides and peroxy acids, leading to higher SOA yields (Johnson et al., 2005). RO₂+NO₂ reactions have not been considered as important for SOA formation due to the short lifetime of peroxy nitrates (< 1 s); the notable exceptions are acyl peroxy nitrates (PANs) and pernitric acid (PNA). As a result, the so-called “high-NO_x” yields (corresponding to urban NO_x levels) have typically been measured under high-NO conditions. For example, the overall SOA mass yield for isoprene photooxidation ranges from 0.01–0.05 under low-NO_x conditions (Kroll et al., 2006) to 0.002–0.03 under high-NO_x (high-NO) conditions (Kroll et al., 2005a; Dommen et al., 2006). Owing to the large emissions of isoprene (Guenther et al., 2006), isoprene has been estimated to be the single largest source of SOA globally (Henze and Seinfeld, 2006; Carlton et al., 2009).

In a recent study of the mechanism of SOA formation from isoprene, it was shown that aerosol-phase 2-methylglyceric acid (2-MG) and its oligoesters are produced from methacrolein oxidation through the peroxy methacryloyl nitrate (MPAN) channel, as the SOA from MPAN oxidation is similar in composition to that from high-NO_x oxidation of isoprene and methacrolein (Surratt et al., 2010). Since MPAN is formed from the reversible reaction of methacryloyl peroxy radicals with NO₂, SOA formation can be highly sensitive to the NO₂ concentration, an effect of gas-phase aldehyde chemistry that had previously not been recognized. Given the large emissions and the substantial fraction of isoprene reacting under high-NO_x conditions (a recent modeling study predicts that globally up to two-thirds of isoprene reacts under high-NO_x conditions (Paulot et al., 2009)), it is essential to understand more generally how gas-phase aldehyde chemistry and both NO and NO₂ affect SOA yield and composition. Here we present the results of a systematic study of the effect of NO₂/NO ratio on SOA formation from methacrolein and two other α, β-unsaturated aldehydes, acrolein and crotonaldehyde. In addition, other structurally similar aldehydes and alcohols are studied to provide insight

Table 1. Hydrocarbons studied.

Name	Structure	OH rate constant, cm ³ molec ⁻¹ s ⁻¹
isoprene		1 × 10 ⁻¹⁰ ^a
methacrolein		2.9 × 10 ⁻¹¹ ^a
acrolein		2.0 × 10 ⁻¹¹ ^b
crotonaldehyde (<i>cis</i> and <i>trans</i>)		3.5 × 10 ⁻¹¹ ^b
2-methyl-2-butenal (2M2B)		unknown
3-methyl-2-butenal (3M2B)		6.2 × 10 ⁻¹¹ ^c
2-pentenal		unknown
4-pentenal		unknown
2-methyl-3-buten-1-ol (MBO231)		unknown
2-methyl-3-buten-2-ol (MBO232)		3.9 × 10 ⁻¹¹ ^d

^a Atkinson and Arey (2003); ^b Magneron et al. (2002); ^c Tuazon et al. (2005); ^d Fantechi et al. (1998).

into the reaction mechanism and to establish the role of PAN-type compounds as important SOA intermediates.

2 Experimental section

2.1 Experimental protocols

Experiments were carried out in the Caltech dual 28-m³ Teflon chambers. Details of the facilities have been described previously (Cocker et al., 2001; Keywood et al., 2004). Before each experiment, the chambers were flushed with dried purified air for >24 h (~4–6 air changes), until the particle number concentration <100 cm⁻³ and the volume concentration <0.1 μm³ cm⁻³. In all experiments, inorganic seed particles were injected by atomization of a 0.015 M aqueous ammonium sulfate solution. The parent hydrocarbon was then introduced into the chamber by injecting a known volume of the liquid hydrocarbon into a glass bulb, and the vapor was carried into the chamber with 5 L min⁻¹ of purified air.

Table 2. Experimental conditions and results.

Date ^a (DD/MM/YY)	Compound	[HC] ₀ , ppb	OH precursor	NO _x addition	[NO] ₀ ^b , ppb	[NO ₂] ₀ ^b , ppb	NO ₂ /NO ^c	V ₀ ^d , μm ³ cm ⁻³	ΔM ₀ ^e , μg m ⁻³	SOA Yield
14/07/09	methacrolein	277	HONO	+NO	725	365	0.5	11.4	10.1	0.019
16/07/09	methacrolein	285	HONO	+NO ₂	296	692	1.7	12.3	24.5	0.052
19/07/09	methacrolein	257	HONO	–	527	407	0.7	12.1	14.4	0.030
31/07/09 ^f	methacrolein	232	HONO	+NO	653	394	0.5	11.7	13.3	0.030
12/09/09	methacrolein	255	CH ₃ ONO	+NO+NO ₂	222	799	10.0	13.9	276.3	0.392
15/09/09	methacrolein	67	CH ₃ ONO	+NO+NO ₂	164	549	5.8	14.8	39.9	0.211
17/09/09	methacrolein	20	CH ₃ ONO	+NO+NO ₂	170	602	3.6	16.0	10.8	0.194
19/09/09	methacrolein	48	CH ₃ ONO	+NO+NO ₂	167	582	4.7	13.2	28.8	0.213
21/09/09	methacrolein	32	CH ₃ ONO	+NO+NO ₂	176	657	4.2	14.4	22.4	0.242
16/12/09	methacrolein	32	CH ₃ ONO	+NO+NO ₂	243	444	2.7	13.9	6.8	0.079
17/12/09 ^g	methacrolein	32	CH ₃ ONO	+NO+NO ₂	233	518	2.7	16.2	6.7	0.075
08/08/09	isoprene	523	HONO	–	312	510	7.7	10.8	65.2	0.044
23/09/09	isoprene	228	CH ₃ ONO	+NO+NO ₂	293	825	8.4	16.0	47.4	0.074
24/09/09	isoprene	94	CH ₃ ONO	+NO+NO ₂	271	735	5.0	14.8	16.0	0.061
25/09/09	isoprene	153	CH ₃ ONO	+NO+NO ₂	316	859	6.1	18.7	27.2	0.064
27/09/09	isoprene	44	CH ₃ ONO	+NO+NO ₂	259	715	4.0	15.8	5.2	0.042
30/09/09	isoprene	33	CH ₃ ONO	+NO+NO ₂	289	768	3.4	18.4	2.9	0.031
15/08/09	acrolein	676	HONO	–	214	389	2.5	13.2	21.3	0.022
16/08/09	acrolein	540	HONO	+NO	550	359	0.8	11.2	4.4	0.006
17/08/09	acrolein	611	HONO	+NO ₂	233	630	2.0	13.2	9.9	0.015
28/09/09	acrolein	220	CH ₃ ONO	+NO+NO ₂	313	830	5.5	19.2	16.6	0.035
18/08/09	crotonaldehyde	293	HONO	–	214	371	2.3	12.1	14.0	0.019
19/08/09	crotonaldehyde	297	HONO	+NO	600	416	1.1	12.3	9.0	0.013
20/08/09	crotonaldehyde	361	HONO	+NO ₂	245	625	2.6	12.2	12.9	0.017
29/09/09	crotonaldehyde	74	CH ₃ ONO	+NO+NO ₂	248	664	3.8	16.4	9.2	0.044
26/12/09	2-pentenal	174	CH ₃ ONO	+NO+NO ₂	230	548	6.7	13.9	18.1	0.03
27/12/09	4-pentenal	191	CH ₃ ONO	+NO+NO ₂	243	488	6.5	15.8	8.2	0.012
28/12/09	2M2B	277	CH ₃ ONO	+NO+NO ₂	240	706	9.3	13.8	376.7	0.391
29/12/09	3M2B	207	CH ₃ ONO	+NO+NO ₂	268	747	8.7	16.1	5.6	0.008
31/12/09	MBO231	589	CH ₃ ONO	+NO+NO ₂	308	493	13.2	16.8	87.6	0.042
22/02/10	MBO231	329	CH ₃ ONO	+NO+NO ₂	351	768	7.8	14.5	21.9	0.019
24/02/10	MBO231	300	HONO	+NO	642	514	1.8	14.2	<2	<0.002
25/02/10	MBO231	378	CH ₃ ONO	+NO+NO ₂	346	793	5.5	17.5	10.7	0.008
01/01/10	MBO232	492	CH ₃ ONO	+NO+NO ₂	251	442	11.4	14.8	<2	<0.002
23/02/10	MBO232	388	CH ₃ ONO	+NO+NO ₂	345	809	8.4	17.1	<2	<0.002

^a All experiments carried out at temperatures of 293–295 K and RH of 9–11%. ^b As measured by chemiluminescence NO_x monitor. Note interference on NO₂ signal from HONO and CH₃ONO. ^c Estimated by photochemical modeling (see Appendix). ^d V₀: volume concentration of ammonium sulfate seed. ^e ΔM₀: mass concentration of SOA. ^f Gas-phase nitric acid added during experiment. ^g Low O₂ experiment.

To study the sensitivity of aerosol yields and composition to relative concentrations of NO and NO₂, different OH precursors were used. Use of nitrous acid (HONO) and methyl nitrite (CH₃ONO) as OH precursors allows for SOA yield measurements over a wide range of NO₂/NO ratios. For “high NO” experiments, OH radicals were generated from photolysis of HONO. We refer to these experiments as “high NO” experiments because NO concentrations are sufficiently high that RO₂+NO ≫ RO₂+NO₂, most notably for acyl peroxy radicals, even though NO₂ concentrations are high (>100 ppb). HONO was prepared by adding 15 mL of 1 wt% aqueous NaNO₂ dropwise into 30 mL of 10 wt% sulfuric acid in a glass bulb. A stream of dry air was then passed through the bulb, sending HONO into the chamber. During this process, NO and NO₂ formed as side products and were also introduced into the chamber. To achieve high NO₂

concentrations, CH₃ONO was employed as the OH precursor. These experiments are referred to as “high NO₂” experiments, as NO₂ concentrations are sufficiently higher than NO concentrations such that PAN formation is favored over reaction of acyl peroxy radicals with NO. CH₃ONO was vaporized into an evacuated 500 mL glass bulb and introduced into the chamber with an air stream of 5 L min⁻¹. The mixing ratio of CH₃ONO injected was estimated to be 200–400 ppb, based on the vapor pressure in the glass bulb measured using a capacitance manometer (MKS). In all experiments, varying amounts of NO and NO₂ were also added from gas cylinders (Scott Marrin) both to ensure high-NO_x conditions and to vary the NO₂/NO ratio. For the C₅ unsaturated aldehydes and 2-methyl-3-buten-2-ol (MBO232), only high NO₂ experiments were conducted. Abbreviations, structures, and OH rate constants (Atkinson and Arey, 2003; Magneron et al.,

2002; Tuazon et al., 2005; Fantechi et al., 1998) of the compounds studied are listed in Table 1, and initial conditions of the experiments are summarized in Table 2.

2.2 Materials

The parent hydrocarbons studied and their stated purities are as follows: isoprene (Aldrich, 99%), methacrolein (Aldrich, 95%), acrolein (Fluka, $\geq 99\%$), crotonaldehyde (Aldrich, 98%, predominantly *trans*), trans-2-pentenal (Alfa Aesar, 96%), 4-pentenal (Alfa Aesar, 97%), trans-2-methyl-2-butenal (Aldrich, 96+%), 3-methyl-2-butenal (Sigma-Aldrich, 97%), 2-methyl-3-buten-1-ol (Aldrich, 98%), and 2-methyl-3-buten-2-ol (Aldrich, 98%). CH₃ONO was synthesized following the method described by Taylor et al. (1980). 9 g of NaNO₂ was added to a mixture of 50 mL of methanol and 25 mL of water. 25 mL of 50 wt% sulfuric acid solution was added dropwise into the solution. The CH₃ONO vapor was carried in a small stream of ultra high purity N₂ through a concentrated NaOH solution and an anhydrous CaSO₄ trap to remove any sulfuric acid and water, respectively. The CH₃ONO was then collected in a cold trap immersed in a dry ice/acetone bath ($-80\text{ }^{\circ}\text{C}$) and stored under liquid N₂ temperature.

2.3 Measurements

Aerosol size distribution, number and volume concentrations were measured with a differential mobility analyzer (DMA, TSI, 3081) coupled with a condensation nuclei counter (TSI, CNC-3760). The volume concentration was corrected for particle wall loss by applying size-dependent first-order loss coefficients, obtained in a separate seed-only experiment, using methods described in Keywood et al. (2004). Aerosol volume concentrations are converted to mass concentrations assuming a density of 1.4 g cm^{-3} (Kroll et al., 2005a). Concentrations of isoprene, methacrolein, methyl vinyl ketone (MVK), acrolein, and crotonaldehyde were monitored using a gas chromatograph with flame ionization detector (GC/FID, Agilent 6890N), equipped with an HP-PLOT Q column (15 m \times 0.53 mm ID \times 30 μm thickness, J&W Scientific). For 2M2B, 3M2B, 2-pentenal, 4-pentenal, MBO231 and MBO232 experiments, the GC/FID was equipped with an HP-5 column (15 m \times 0.53 mm ID \times 1.5 μm thickness, Hewlett Packard). A commercial chemiluminescence NO/NO_x analyzer (Horiba, APNA 360) was used to monitor NO and NO_x. Both HONO and CH₃ONO produce interference on the NO₂ signal from the NO_x monitor. Concentrations of NO and NO₂ are estimated by photochemical modeling (see Appendix). Temperature, RH, and ozone (O₃) were continuously monitored.

A custom-modified Varian 1200 triple-quadrupole chemical ionization mass spectrometer (CIMS) was used to continuously monitor gas-phase species over each experiment. Details of the operation of the CIMS can be found in a num-

ber of previous reports (Crouse et al., 2006; Paulot et al., 2009). The CIMS was operated in negative ion mode, in which CF₃O⁻ is used as the reagent ion, and in positive ion mode of proton transfer mass spectrometry (PTR-MS). In the negative mode, the reagent ion CF₃O⁻ clusters with the analyte, R, forming ions at mass-to-charge ratios (m/z) MW+85 (R \cdot CF₃O⁻), or, with more acidic species, at m/z MW+19 (HF \cdot R_{-H}⁻). In the positive mode, positively charged water clusters, $n(\text{H}_2\text{O})\text{H}^+$, react via proton transfer with the analyte, R, to form the positively charged ion, R \cdot $n(\text{H}_2\text{O})\cdot\text{H}^+$. In some cases, tandem mass spectrometry (MS/MS) was used to separate isobaric compounds. In brief, the parent ions selected in the first quadrupole undergo collision-induced dissociation (CID) in the second quadrupole. The parent ions of isobaric compounds can exhibit different CID patterns and yield different daughter ions. Hence, with the third quadrupole acting as a second mass filter for the daughter ions, this allows for separate measurement of these isobaric compounds (see Supplementary Material). The significance of this separation will be discussed in a later section.

Real-time particle mass spectra were collected continuously by an Aerodyne High Resolution Time-of-Flight Aerosol Mass Spectrometer (DeCarlo et al., 2006; Canagaratna et al., 2007), hereby referred to as the AMS. The AMS switched once every minute between the high resolution “W-mode” and the lower resolution, higher sensitivity “V-mode”. The “V-mode” data were analyzed using a fragmentation table to separate sulfate, ammonium, and organic spectra and to time-trace specific mass-to-charge ratios. “W-mode” data were analyzed using a separate high-resolution spectra toolbox known as PIKA to determine the chemical formulas contributing to distinct m/z ratios (DeCarlo et al., 2006).

Aerosol samples were also collected on Teflon filters and analyzed by offline mass spectrometry. Detailed sample collection and extraction protocol are described in Surratt et al. (2008). Filter extraction using 5 mL of high-purity methanol (i.e., LC-MS Chromasolv Grade) was performed by 45 min of sonication. The filter extracts were then analyzed by a Waters ACQUITY ultra performance liquid chromatography (UPLC) system, coupled with a Waters LCT Premier TOF mass spectrometer equipped with an ESI source operated in the negative (–) mode, allowing for accurate mass measurements (i.e., determination of molecular formulas) to be obtained for each observed ion. Operation conditions and parameters for the UPLC/(–)ESI-TOFMS measurement have been described by Surratt et al. (2008).

3 SOA formation

The importance of isoprene as an SOA source was suggested by identification of 2-methyltetrols and 2-methylglyceric acid (2-MG) in both ambient POM (Claeys et al., 2004; Edney et al., 2005; Ion et al., 2005; Kourtchev et al., 2005)

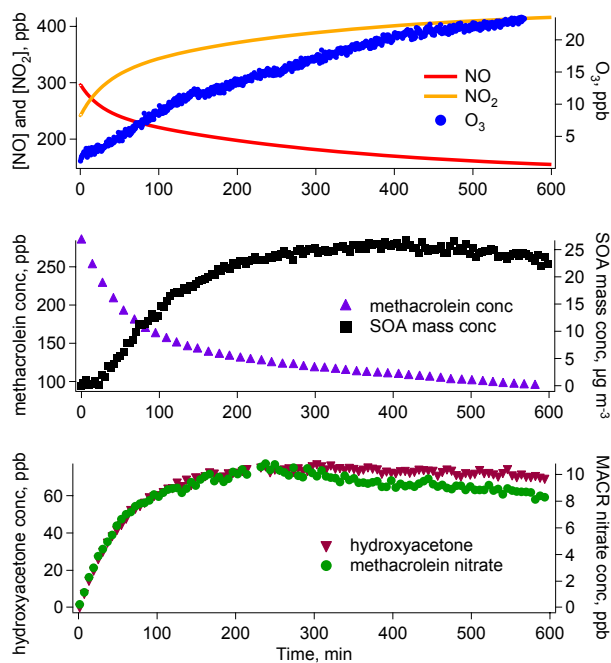


Fig. 1. Concentration profiles of gas-phase species during a typical methacrolein/high-NO experiment (16/07/09). In this experiment, additional NO₂ was injected prior to irradiation. Concentrations of NO and NO₂ shown here are calculated from a photochemical model (see Appendix).

and laboratory aerosol generated from isoprene photooxidation (Edney et al., 2005; Surratt et al., 2006; Szmigielski et al., 2007; Kleindienst et al., 2009). Methacrolein, a first-generation oxidation product of isoprene, has been shown to produce SOA upon further oxidation (Kroll et al., 2006; Surratt et al., 2006) and has been identified as the precursor to aerosol-phase 2-MG and its corresponding oligoester products (Surratt et al., 2006; Szmigielski et al., 2007). A recent study shows aerosol formation from methacrolein oxidation proceeds via subsequent oxidation of MPAN (Surratt et al., 2010). Here we focus our attention on photooxidation of methacrolein under high-NO_x conditions to establish the effect of relative NO and NO₂ concentrations on SOA yields and composition. Acrolein, crotonaldehyde, 2-methyl-2-butenal (2M2B), 3-methyl-2-butenal (3M2B), 2-pentenal, and 4-pentenal differ from methacrolein by one or two methyl groups, and studying their SOA formation provides insight into the mechanism of formation of low-volatility products. Furthermore, aerosol formation from photooxidation of 2-methyl-3-buten-2-ol (MBO232), an atmospherically important unsaturated alcohol (Harley et al., 1998), and structurally similar 2-methyl-3-buten-1-ol (MBO231) is studied to investigate the role of PAN-like compounds in SOA formation.

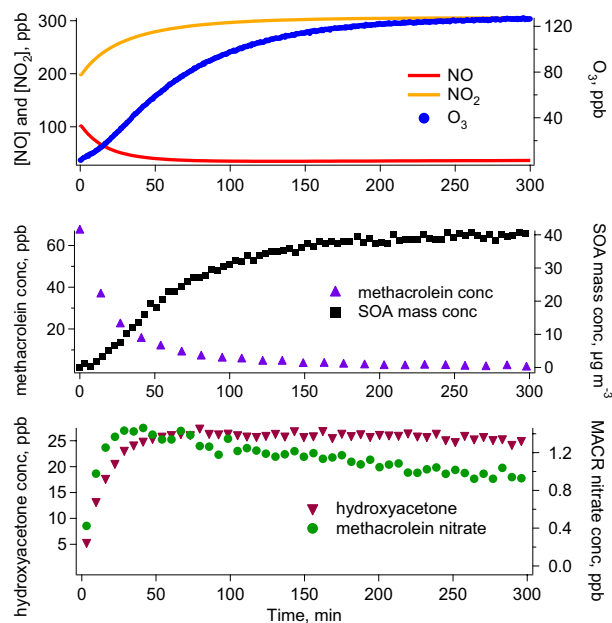


Fig. 2. Concentration profiles of gas-phase species during a typical methacrolein/high-NO₂ experiment (15/09/09). Additional NO (100 ppb) and NO₂ (200 ppb) were injected prior to irradiation. Concentrations of NO and NO₂ shown here are calculated from a photochemical model (see Appendix). As a result of the higher OH concentrations from CH₃ONO than from HONO, more methacrolein was reacted and the concentrations of methacrolein nitrate relative to those of hydroxyacetone were lower than those in high-NO experiments, owing to a more rapid consumption by OH.

3.1 Methacrolein

Figures 1 and 2 show typical concentration profiles of various gas-phase species in methacrolein/HONO (high NO) and methacrolein/CH₃ONO (high NO₂) photooxidation experiments, respectively. In all experiments, NO concentrations remain above 50 ppb during SOA growth, at which conditions RO₂+HO₂ or RO₂+RO₂ reactions are not competitive with those of RO₂ with NO and NO₂. Products of these reactions, such as methacrylic acid and methacrylic peracid, are not observed by CIMS. Instead, hydroxyacetone and methacrolein nitrate, products from RO₂+NO reactions, are observed. During these experiments, RO₂ and HO₂ produced from methacrolein oxidation react with NO to produce NO₂, which photolyzes to form ozone. As a result, ozone concentrations reach a maximum of up to 126 ppb. Despite relatively high levels of ozone, reaction rates of methacrolein and peroxy methacryloyl nitrate (MPAN) with ozone are still slow compared to those with OH, as efficient photolysis of HONO or CH₃ONO leads to OH concentrations > 3 × 10⁶ molec cm⁻³, estimated from the methacrolein decay. For high-NO experiments, the initial decay of methacrolein slows down after 5 h, consistent with the HONO signal (CIMS (–) *m/z* 66) approaching zero. In

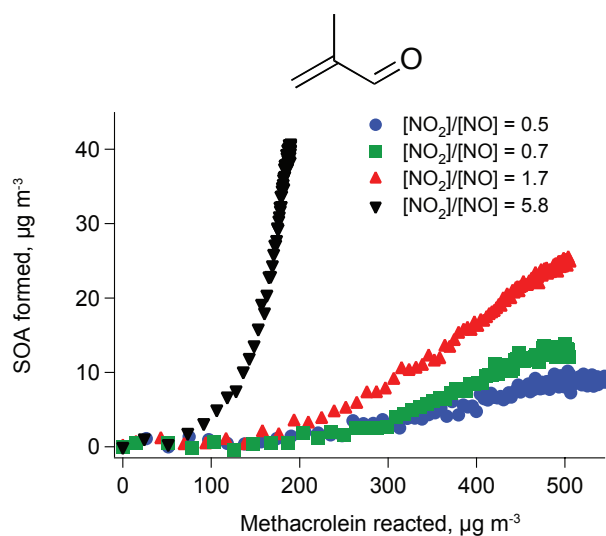


Fig. 3. Time-dependent SOA growth curves for methacrolein photooxidation. NO₂/NO ratios are computed from photochemical modeling (see Appendix). In the high-NO experiments (NO₂/NO < 2) HONO was used as the OH precursor, and the NO₂/NO ratio was varied by adding different amounts of NO or NO₂. In the high-NO₂ experiment (black triangles), CH₃ONO was used as the OH precursor.

these experiments, more than 70% of the initial methacrolein is consumed before SOA growth ceases. In the high-NO₂ experiments, more than 90% of the initial methacrolein is consumed before SOA growth ceases.

Mass concentrations of SOA versus the concentration of methacrolein reacted, so-called “time-dependent growth curves”, are shown in Fig. 3. As reported previously, under high-NO conditions (with HONO as the OH precursor), when additional NO is added before irradiation, aerosol formation (mass yield of 0.019) from photooxidation of 277 ppb of methacrolein is suppressed (Surratt et al., 2010). In contrast, SOA yields are higher when no additional NO is added (0.030 from 257 ppb methacrolein), and the highest when 350 ppb of additional NO₂ (instead of NO) is injected (0.052 from 285 ppb methacrolein) (Surratt et al., 2010). In all high-NO experiments, the NO₂/NO ratio remains low (< 2), owing to presence of NO impurity in HONO synthesis and production of NO during HONO photolysis. The observed dependence of SOA yields on NO₂/NO ratio is not a result of condensation of nitric acid from OH+NO₂, as the experiments were conducted under dry (< 10% RH) conditions. In confirmation of this conclusion, addition of gas-phase nitric acid in one experiment (31/07/09) did not lead to additional aerosol growth.

In the high-NO₂ experiments, CH₃ONO was used as the OH precursor and lower NO concentrations are expected, owing to relatively pure CH₃ONO synthesis and no net production of NO from CH₃ONO photolysis (see Appendix). Higher SOA yields are observed at higher NO₂/NO ratios;

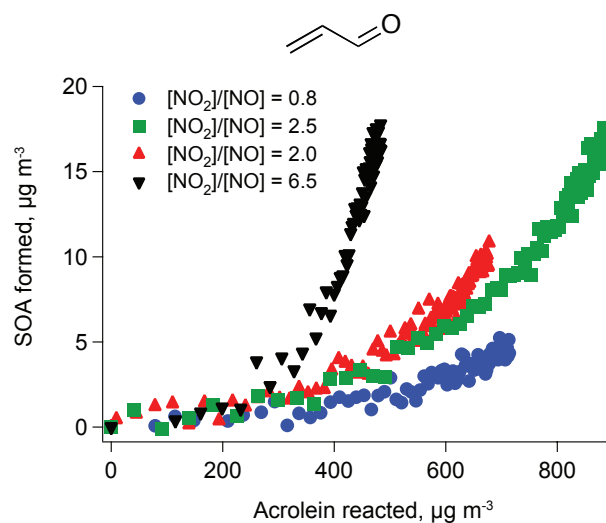


Fig. 4. Time-dependent SOA growth curves for acrolein photooxidation. Similar to methacrolein photooxidation, NO₂/NO ratios are computed from photochemical modeling (see Appendix). In the high-NO experiments (NO₂/NO < 3), HONO was used as the OH precursor, and the NO₂/NO ratio was varied by adding different amounts of NO or NO₂. In the experiment in which NO₂ was added (red triangles), high levels of NO₂ depress OH concentrations, resulting in less acrolein reacted. Concentrations of NO did not drop as rapidly as in other high-NO experiments, leading to a lower NO₂/NO ratio. In the high-NO₂ experiment (black triangles), CH₃ONO was used as the OH precursor.

correspondingly, much lower concentrations of methacrolein are required to produce the same amount of SOA (see Fig. 3). Also, owing to the high concentrations of CH₃ONO injected, more than 90% of the initial methacrolein is consumed before CH₃ONO is depleted. For example, when 255 ppb of initial methacrolein is oxidized using CH₃ONO as OH precursor (12/09/09), the SOA yields are more than 5 times larger than when a similar amount of methacrolein is reacted using HONO as OH precursor. This rules out a larger extent of reaction as the cause of the high observed SOA yields. HO₂ concentrations, quantified from the pernitric acid signal on the CIMS ((-) *m/z* 98) and modelled NO₂ concentrations, do not exceed 60 ppt in all experiments. At organic loadings of 10–20 µg m⁻³, SOA mass yields of methacrolein/high-NO₂ and methacrolein/high-NO photooxidation are roughly 0.19 and 0.03, respectively.

3.2 Acrolein and crotonaldehyde

Figures 4 and 5 show SOA growth curves for acrolein and crotonaldehyde photooxidation, respectively. The SOA yields of these compounds are lower than those of methacrolein, with maximum yields of roughly 0.08 at the highest loadings (> 100 µg m⁻³). These compounds exhibit a similar dependence of SOA growth on NO₂/NO ratio to that of methacrolein: SOA formation is suppressed with addition

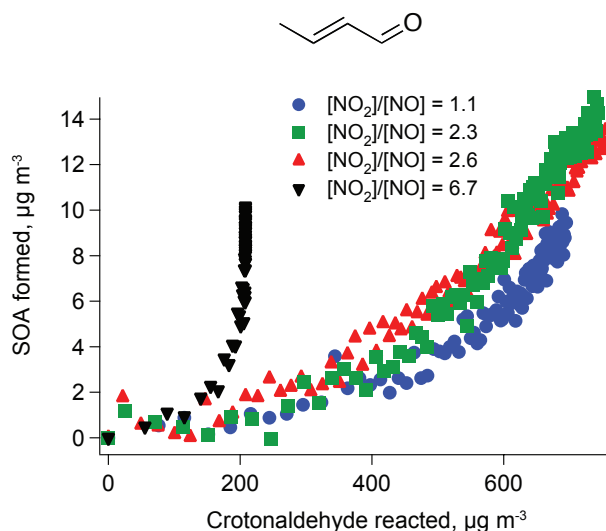


Fig. 5. Time-dependent SOA growth curves for crotonaldehyde photooxidation. Similar to methacrolein photooxidation, NO₂/NO ratios are computed from photochemical modeling (see Appendix). In the high-NO experiments (NO₂/NO < 3), HONO was used as the OH precursor, and the NO₂/NO ratio was varied by adding different amounts of NO or NO₂. In the high-NO₂ experiment (black triangles), CH₃ONO was used as the OH precursor.

of NO, and enhanced with addition of NO₂. SOA yields are highest in the high-NO₂ experiments. Oxidation products analogous to those found in the methacrolein system, such as glycolaldehyde and hydroxynitrates, are observed in the gas phase at similar yields.

3.3 Other aldehydes and methylbutenols (MBO)

The growth curves for 2M2B and 3M2B photooxidation are shown in Fig. 6. Significant SOA growth is observed for 2M2B (277 ppb) photooxidation under high-NO₂ conditions, with mass yields exceeding 0.35. Similar to methacrolein, 2M2B contains a methyl group in the α -position. Interestingly, photooxidation of 3M2B under similar NO_x conditions and hydrocarbon loadings (207 ppb), produces less SOA (mass yield < 0.01). 3M2B is a structural isomer of 2M2B with the methyl group in the β -position. The trend in SOA yields between 2M2B and 3M2B is consistent with that observed for methacrolein and crotonaldehyde, their C₄ analogs. The SOA yields from 2-pentenal, a straight-chain α,β -unsaturated aldehyde, are higher than those from 4-pentenal, in which the olefinic bond is not adjacent to the aldehyde group (see Fig. 6).

We also carried out MBO232 and MBO231 photooxidation under high-NO₂ conditions. Both MBO's are structurally similar to isoprene and, upon high-NO_x photooxidation, produce an aldehyde (i.e., hydroxy-methylpropanal, HMPR) analogous to methacrolein. Previous results have shown that aerosol formation from MBO232 photooxidation

under high-NO conditions is negligible, with mass yields of < 0.001 (Carrasco et al., 2007; Chan et al., 2009a). Here we do not observe SOA growth even at high NO₂/NO ratios. Gas-phase compounds such as glycolaldehyde and HMPR are observed at molar yields of 0.6 and 0.3, respectively, consistent with those published in previous product studies (Carrasco et al., 2007; Chan et al., 2009a). On the other hand, MBO231, a structural isomer with the hydroxyl group in the 1-position, produces a significant amount of SOA (mass yields of 0.008–0.042) upon oxidation under high-NO₂ conditions, comparable to that of isoprene under similar conditions (see Fig. 6). Under high-NO conditions, no SOA is formed. The dependence of SOA yields from MBO231 on NO₂/NO ratio is therefore consistent with that observed in unsaturated aldehydes.

4 Chemical composition of SOA

4.1 Offline chemical analysis

In previous work, offline chemical analysis of SOA from photooxidation of isoprene, methacrolein, and MPAN by UPLC/(–)ESI-TOFMS has been presented (Surratt et al., 2010). The same compounds are detected in the methacrolein experiments in this work under both high-NO and high-NO₂ conditions, and are summarized in Table 3. Four series of oligoester products from 2-methylglyceric acid (2-MG) and C₄-hydroxynitrooxycarboxylic acid are identified in the SOA. The compounds in the 2-MG oligoester series differ by 102 Da, corresponding to esterification of a 2-MG monomer unit (Surratt et al., 2006). The accurate masses of the identified ions confirm their elemental compositions, and their structures are proposed based on detailed characterization by tandem MS and GC/MS analyses with prior trimethylsilylation (Szmigielski et al., 2007).

All ions detected by UPLC/(–)ESI-TOFMS in acrolein and crotonaldehyde SOA are listed in the Supplementary Material. It is noteworthy that the identities of detected aerosol-phase products are the same regardless of the OH precursor used. The ions detected in acrolein SOA differ from those found in methacrolein SOA by one methyl group for every monomer unit, and those detected in crotonaldehyde SOA have the same exact mass and elemental composition as those in methacrolein SOA. Detected [M-H][–] ions in SOA from 2M2B and 2-pentenal can also be found in the Supplementary Material. No filter sample was collected for 3M2B owing to low aerosol loading. Aerosol-phase products of methacrolein, acrolein, crotonaldehyde, 2M2B and 2-pentenal are structural analogs of each other, and the structures for the deprotonated ions are proposed based on those characterized previously in isoprene and methacrolein SOA (Surratt et al., 2006; Szmigielski et al., 2007). Interestingly, SOA produced from 4-pentenal is composed of entirely different products, and hence no structures are proposed at this

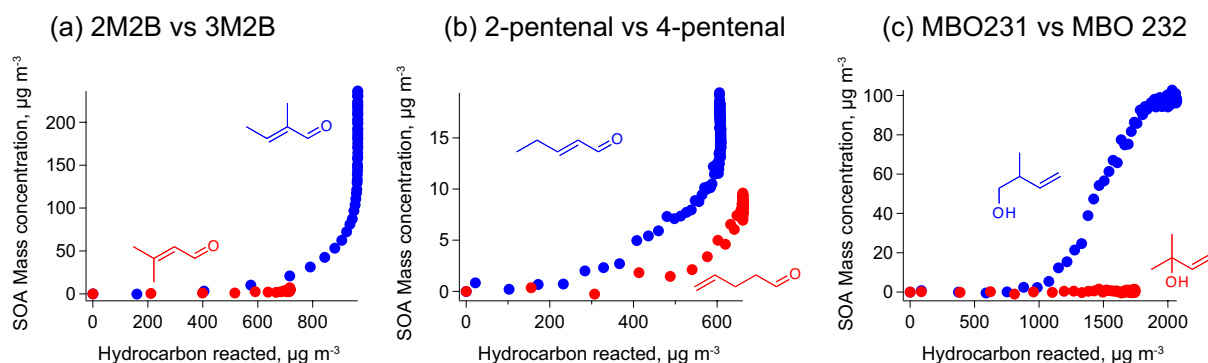


Fig. 6. Comparisons of time-dependent SOA growth from photooxidation of (a) 2M2B and 3M2B, (b) 2-pentenal and 4-pentenal, and (c) MBO232 and MBO 231 under high-NO₂ conditions. Within each plot, initial concentrations of parent hydrocarbons are comparable (see Table 2).

Table 3. SOA constituents detected by UPLC/(–)ESI-TOFMS and AMS in methacrolein experiments. All ions were detected in both high-NO and high-NO₂ experiments, unless otherwise noted.

	UPLC/ESI-TOFMS Measured Mass	TOFMS Suggested Ion Formula	Error (mDa)	i-Fit	# of 2-MG Monomer Units (<i>n</i>)	Structure	AMS Suggested Ion Formula ^c
	[M – H] ^{–a}						[M – OH] ^{+b}
		not detected			1		103
Oligoester Series 1	221	221.0661	C ₈ H ₁₃ O ₇ [–]	1.6	0.3	2	205
	323	323.0979	C ₁₂ H ₁₉ O ₁₀ [–]	0.1	22.6	3	^d –
	425	425.1290	C ₁₆ H ₂₅ O ₁₃ [–]	–0.5	48.0	4	^d –
	527 ^e	527.1609	C ₂₀ H ₃₁ O ₁₆ [–]	–0.3	3.7	5	^d –
Oligoester Series 2	266	266.0507	C ₈ H ₁₂ NO ₉ [–]	–0.5	32.8	1	^d –
	368	368.0831	C ₁₂ H ₁₈ NO ₁₂ [–]	0.2	11.4	2	^d –
	470	470.1149	C ₁₆ H ₂₄ NO ₁₅ [–]	0.3	56.3	3	^d –
	572	572.1510	C ₂₀ H ₃₀ NO ₁₈ [–]	4.7	1.0	4	^d –
Oligoester Series 3 ^f		not detected			1		131
	249	249.0616	C ₉ H ₁₃ O ₈ [–]	0.6	2.7	2	233
	351	351.0912	C ₁₃ H ₁₉ O ₁₁ [–]	–1.5	46.9	3	^d –
	453	453.1248	C ₁₇ H ₂₅ O ₁₄ [–]	0.4	63.7	4	^d –
	555 ^e	555.1610	C ₂₁ H ₃₁ O ₁₇ [–]	4.9	3.0	5	^d –
Oligoester Series 4 ^g		not detected			1		145
	263	263.0740	C ₁₀ H ₁₅ O ₈ [–]	–2.7	4.7	2	247
	365	365.1061	C ₁₄ H ₂₁ O ₁₁ [–]	–2.3	54.9	3	^d –
	467	467.1434	C ₁₈ H ₂₇ O ₁₄ [–]	3.3	23.7	4	^d –
	569	569.1711	C ₁₈ H ₂₇ O ₁₄ [–]	–0.7	20.0	5	^d –
Oligoester Series 5	311	311.0333	C ₈ H ₁₁ N ₂ O ₁₁ [–]	–3.0	58.9	0	^d –
	413	413.0664	C ₁₂ H ₁₇ N ₂ O ₁₄ [–]	–1.6	71.9	1	^d –
	515 ^e	515.1039	C ₁₆ H ₂₃ N ₂ O ₁₇ [–]	4.2	3.6	2	^d –
Other Oligoesters	458 ^e	458.0558	C ₁₂ H ₁₆ N ₃ O ₁₆ [–]	2.7	3.3	n/a	^d –

^a Observed by UPLC/(–)ESI-TOFMS. ^b Observed by AMS V mode. ^c Suggested by AMS high-resolution W mode.

^d Not observed by AMS, most likely due to fragmentation of nitrate group, or below detection limit. ^e Detected in high-NO₂ experiments only. ^f This oligoester series involves the esterification with formic acid. ^g C₆H₁₁O₃⁺ also detected. ^h This oligoester series involves the esterification with acetic acid.

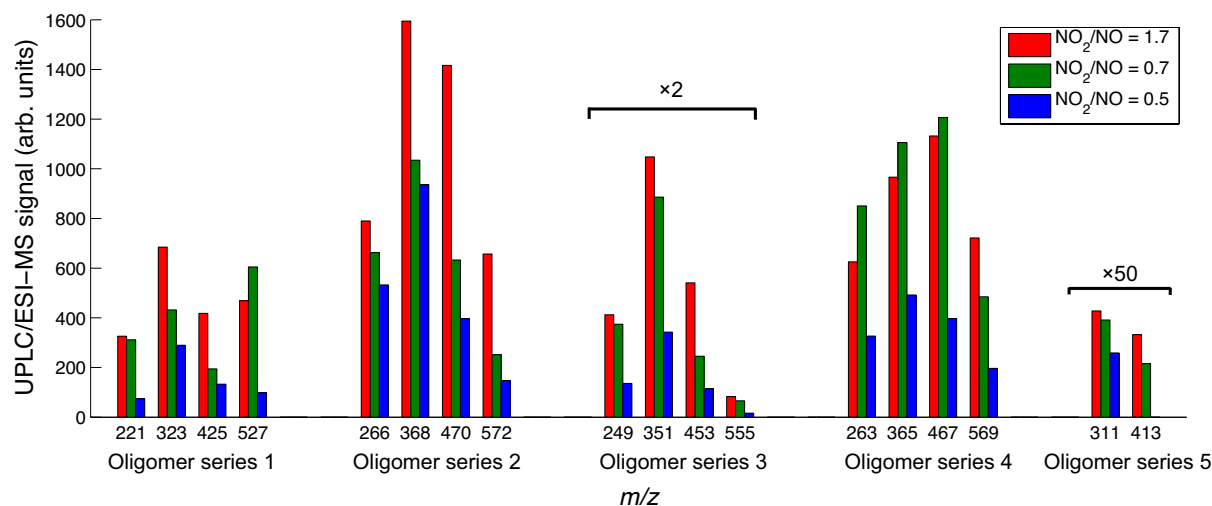


Fig. 7. Absolute peak areas (normalized by sampling volume) of all deprotonated ions detected by UPLC/(-)ESI-TOFMS in methacrolein/high-NO experiments, listed in Table 3. The positive dependence of oligoester abundance on NO₂/NO ratios is consistent with the observed trend in overall SOA growth.

time. The significance of this result will be discussed in a later section.

While the identities of the detected aerosol-phase compounds are independent of the OH precursor, the relative amounts vary greatly and exhibit a strong correlation with NO₂/NO ratio. Figure 7 shows the extracted ion signals for the oligoester products detected by UPLC/(-)ESI-TOFMS in the methacrolein high-NO experiments. The amount of identified aerosol-phase components shows the same dependence on NO₂/NO ratio as the total amount of SOA growth. In general, the abundance of each compound decreases when NO is added and increases when NO₂ is added.

4.2 Online AMS measurements

AMS V-mode organic spectra of SOA from high-NO₂ photooxidation of isoprene and methacrolein are shown in Fig. 8. The mass fragments above m/z 200 likely contain more than 5 carbon atoms, and display a repetitive pattern, indicative of oligomer formation. In addition, 102 Da differences between major peaks were also observed, consistent with previous AMS and LC/MS results (Surratt et al., 2006). Elemental formulas based on accurate mass measurements are determined from high-resolution W-mode data for a number of the major ion peaks observed, as shown in Fig. 9. The ions suggested by these elemental formulas differ from many of the ions detected by UPLC/(-)ESI-TOFMS by an O²⁻ group. The observed AMS ions are consistent with loss of a hydroxyl group from the molecular ion (i.e. α -cleavage of a hydroxyl group under electron impact ionization). In UPLC/(-)ESI-TOFMS, these compounds are detected in their deprotonated form (loss of H⁺). As shown in Table 3, the oligoesters are detected by both online and offline high-resolution mass

spectrometry, and the agreement between the two techniques confirms that the oligoesters identified are indeed present in the SOA, and that the observations by offline aerosol analysis are not the result of filter sampling artifacts. AMS organic spectra of SOA from oxidation of acrolein and crotonaldehyde show similar features, and accurate mass measurements of a number of the major peaks correspond to the products analogous to those found in the methacrolein system (see Supplementary Material).

5 Effect of NO₂/NO ratios on SOA yield and composition

As mentioned in the Introduction, studies on the effect of NO_x concentrations on SOA formation has shown that for most systems, SOA yields are inversely correlated with NO_x concentrations (Hatakeyama et al., 1991; Hurley et al., 2001; Presto et al., 2005; Song et al., 2005; Zhang et al., 2007b; Ng et al., 2007a,b; Chan et al., 2009b). The “NO_x effect” on SOA formation has been described as a competition of the chemistries for RO₂ between HO₂ (the high-yield pathway) and NO (the low-yield pathway), such that the ratio of HO₂ to NO is critical in determining the branching ratio between these two pathways (Kroll and Seinfeld, 2008; Henze et al., 2008). Aerosol yields from isoprene photooxidation are also sensitive to HO₂/NO ratios, with higher yields measured under HO₂-dominated conditions (using H₂O₂ as OH source) (Kroll et al., 2006) than under NO-dominated conditions (using HONO or NO_x cycling as OH source) (Kroll et al., 2005b; Pandis et al., 1991; Dommen et al., 2006). Addition of NO also suppresses SOA growth in low-NO_x experiments, indicating that the RO₂+NO pathway yields

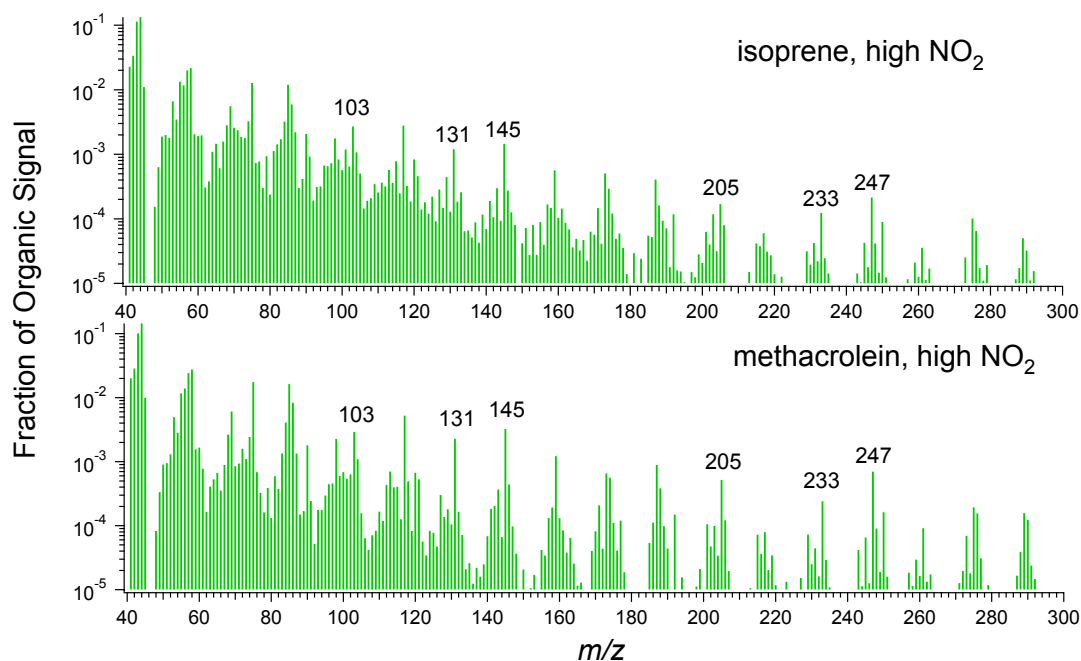


Fig. 8. AMS V-mode organic spectra of SOA from high-NO₂ photooxidation of isoprene and methacrolein. The labelled ion peaks differ from compounds listed in Table 3 by an O²⁻ group. The accurate masses are confirmed by W-mode high-resolution analysis, as shown in Fig. 9. Separation of 102 Da between major peaks is consistent with esterification with a 2-MG monomer.

more volatile products, and hence less SOA (Kroll et al., 2006). However, under the experimental conditions in the present study, RO₂+HO₂ reactions are not expected to be significant. Rather, the dependence of SOA yield on the NO₂/NO ratio is consistent with analysis of SOA composition, which is consistent with MPAN, a product of the acyl peroxy radical+NO₂ reaction, being the intermediate in SOA formation. Although the absolute concentrations of NO₂ in these experiments are a factor of 10 higher than ambient levels, we expect the OH-adduct of alkenes and aldehydes studied here to react predominantly with O₂ to form alkyl peroxy or acyl peroxy radicals. Compounds with nitro functional groups (R-NO₂), such as those found in the aromatic systems (Calvert et al., 2002), were not detected in these experiments.

Based on the proposed mechanism shown in Fig. 10, the acyl peroxy radical formed from abstraction of the aldehydic hydrogen atom of an unsaturated aldehyde react with either NO or NO₂. The reversible reaction of RO₂ with NO₂ forms a PAN-type compound (MPAN for methacrolein), which, in the absence of competing reactions, reaches thermal equilibrium. The irreversible reaction of RO₂ with NO leads to fragmentation into CO₂ and a vinyl radical, which subsequently forms volatile gas-phase products, such as formaldehyde and CO (Orlando et al., 1999). At [OH]=2 × 10⁶ molec cm⁻³, the reaction of MPAN with OH has a rate comparable to that of thermal decomposition (Orlando et al., 2002), and leads to formation of aerosol products. Hence, the SOA formation potential for this system depends critically on the NO₂/NO

ratio. High NO₂/NO ratios shift the thermal equilibrium towards the unsaturated PAN, and SOA formation increases as the fraction of PAN reacting with OH radicals increases. At low NO₂/NO ratios, acyl peroxy radicals react predominantly with NO, leading to relatively volatile products.

Previous measurements of isoprene SOA yields under high-NO_x conditions have been carried out using photolysis of HONO (Kroll et al., 2005a) or the recycling of HO_x and NO_x to generate OH (so-called classical photooxidation) (Pandis et al., 1991; Dommen et al., 2006). Low SOA yields were observed as NO concentrations remained high during the experiments. In fact, SOA growth occurred only after NO concentrations decreased to less than 10 ppb (Kroll et al., 2005a; Dommen et al., 2006). It was proposed that after NO has been consumed, aerosol formation commences as the RO₂+HO₂ pathway becomes competitive. However, such a mechanism is inconsistent with the major differences in composition observed between high- and low-NO_x SOA products. High-NO_x SOA from isoprene photooxidation is dominated by esterification products of C₄-carboxylic acids, whereas under low-NO_x conditions, SOA is dominated by peroxides and C₅-tetrols (Surratt et al., 2006). It is more likely that the decrease in NO concentration (and increase in NO₂ concentration) leads to a transition from an RO₂+NO dominated regime to an RO₂+NO₂ dominated regime, resulting in significant SOA formation via the MPAN route.

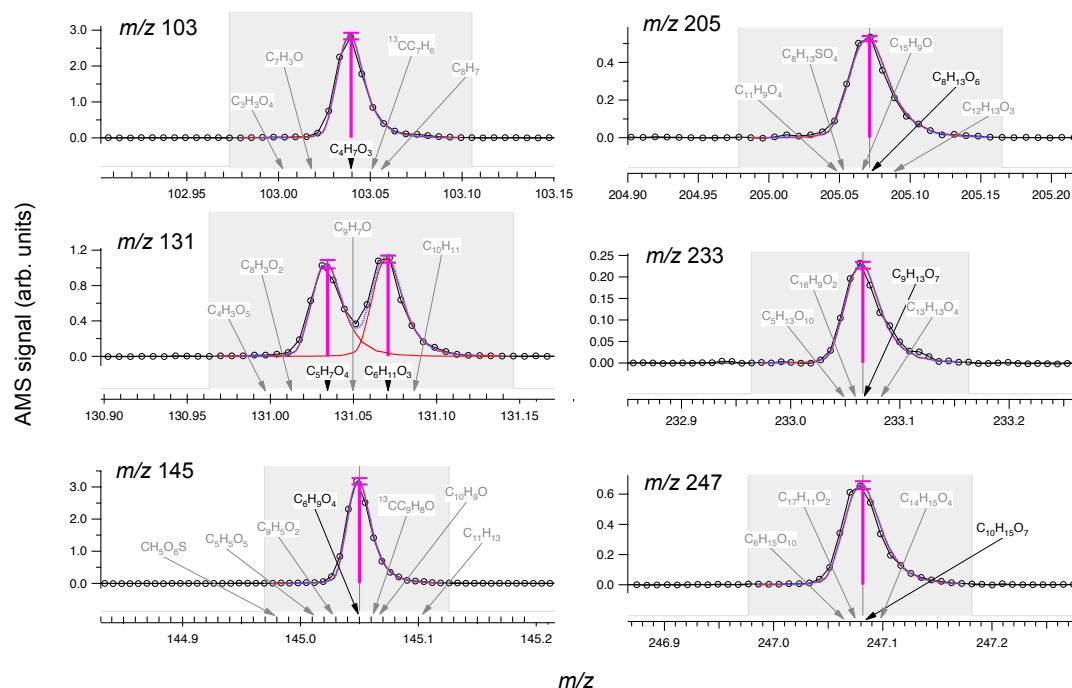


Fig. 9. High-resolution W-mode AMS peaks of a number of the major fragment ions observed in methacrolein/high-NO₂ experiments. Knowledge of the accurate masses allow assignments of molecular formulas, corresponding to loss of hydroxyl groups from compounds detected by offline analysis, suggesting that detection of compounds listed in Table 3 is not a result of sampling artifacts. *m/z* 131 contains two different ions, only one of which is consistent with compounds detected by offline UPLC/(–)ESI-TOFMS analysis.

At NO₂/NO ratios (between 3 and 8) higher than in previous studies (and more relevant to urban conditions), SOA yields from isoprene are approximately 3 times larger than previously measured. The yields even exceed those under low-NO_x conditions at the same organic aerosol loadings, as shown in Fig. 11. This is, in fact, consistent with observations from Kroll et al. (2006) that at very low NO_x concentrations, addition of NO actually increases SOA yield. It is likely that under very low NO concentrations, the NO₂/NO ratio increases rapidly, as NO is quickly converted to NO₂. SOA yields are therefore higher than those in the absence of NO, as RO₂ (from methacrolein)+NO₂ forms SOA more efficiently than RO₂ (from isoprene)+HO₂. However, further increasing NO decreases the NO₂/NO ratio. RO₂ (from methacrolein)+NO becomes more dominant, forms volatile products and leads to a decrease in SOA yield. It must be noted that the effect of RO₂ radical chemistry on SOA formation is complex and can be unique to different systems (Kroll and Seinfeld, 2008). Also, the acidity of the inorganic seed can increase SOA yields significantly: Surratt et al. (2010) shows that SOA yields from isoprene low-NO_x photooxidation can be as high as 0.29. Detailed knowledge of the chemical mechanism is required to predict the effect of NO_x conditions on SOA production.

6 Role of PAN in SOA formation

6.1 Unsaturated aldehydes

One can infer from the shapes of the growth curves the relative timescales of the reaction steps of SOA formation. In all high-NO₂ experiments, a greater extent of reaction is achieved than in high-NO experiments, and SOA formation continues after the parent hydrocarbon is completely consumed; this behavior is characterized by a vertical portion (“hook”) at the end of the SOA growth curve. The presence of this vertical portion indicates that SOA formation results from further reaction of first-generation products, which is the rate-limiting step in the mechanism (see Figs. 3–5). This observation is consistent with our previous results showing that first-generation products of methacrolein, such as hydroxyacetone and MPAN, are themselves still volatile (Surratt et al., 2010). SOA is instead formed from the further OH reaction of MPAN, which has a comparable rate coefficient to that of methacrolein (Orlando et al., 2002).

Formation of dihydroxycarboxylic acids (e.g. 2-MG), hydroxynitrooxycarboxylic acids, and corresponding oligoesters appears to be important SOA formation pathways for the five α,β -unsaturated aldehydes studied here (methacrolein, acrolein, crotonaldehyde, 2M2B, 2-pentenal). All of the SOA constituents detected by offline UPLC/(–)ESI-TOFMS in these systems are structural

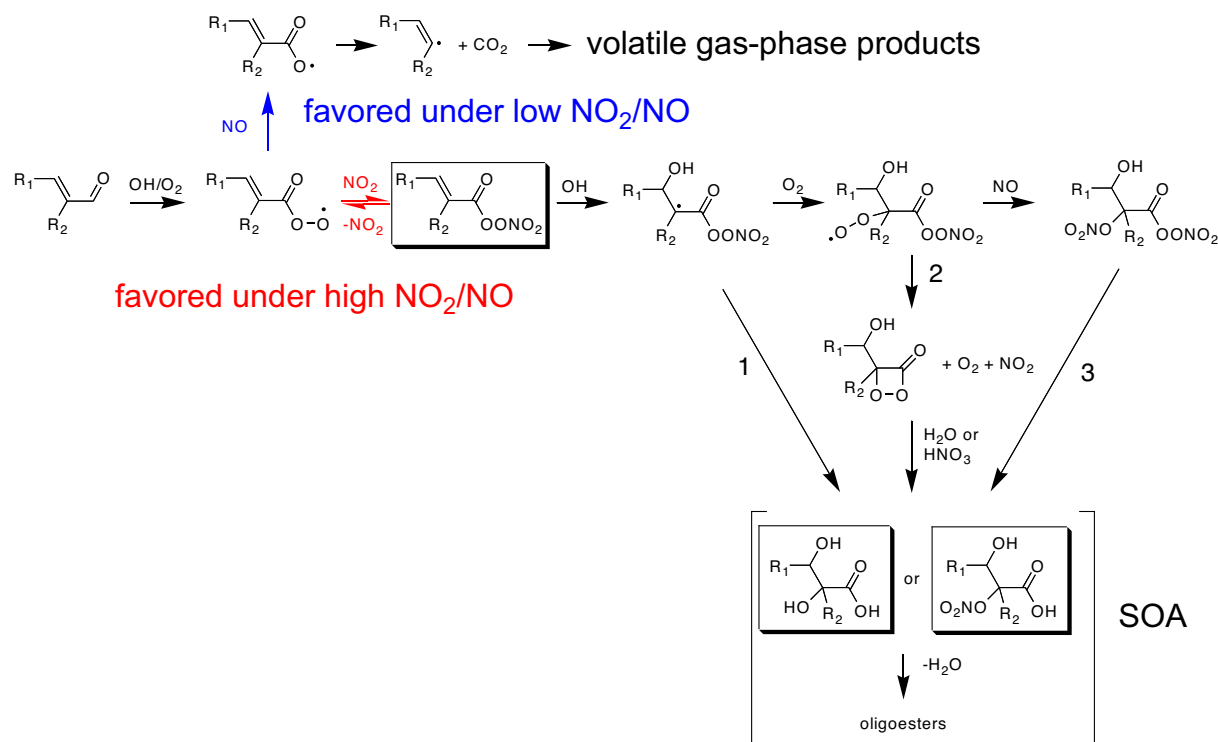


Fig. 10. Proposed mechanism to form aerosol-phase products from α,β -unsaturated aldehydes. The pathways highlighted in red are favored under high NO_2/NO ratios and lead to aerosol formation. The pathways highlighted in blue are favored under low NO_2/NO ratios and lead to fragmentation into volatile products. Aerosol formation from OH-reaction of unsaturated PANs can proceed via 3 possible routes (routes 1–3), and detailed investigation of each route is discussed in the main text.

analogs of each other, as confirmed by the online AMS operated in the high-resolution W-mode. Based on similarities in SOA growth trends and composition, we expect that the formation of SOA products proceeds via pathways similar to those elucidated in Surratt et al. (2010) (see Fig. 10). Although oxidation of these aldehydes can lead to α -dicarbonyls, such as glyoxal and methylglyoxal, which can undergo reactive uptake under humid conditions (Liggio et al., 2005; Kroll et al., 2005b; Volkamer et al., 2009), these compounds are not expected to contribute significantly to SOA formation under dry conditions. In addition, the AMS spectra for acrolein and crotonaldehyde SOA do not show peaks that are characteristic of glyoxal and its oligomers, as described in Liggio et al. (2005) and Galloway et al. (2009).

While MPAN is clearly the intermediate in SOA formation from methacrolein, the exact mechanism by which MPAN leads to such aerosol-phase products as 2-MG and hydroxynitrooxycarboxylic acids has not been established. From the oligoesters observed in the aerosol phase, it appears that the C_4 backbone of MPAN remains intact. Following OH addition to the double bond, the only known gas-phase pathway that would preserve the carbon backbone is formation of hydroxynitrates. (Fragmentation of the MPAN-alkoxy radical would break up the C_4 backbone and yield smaller products.) The nitroxy functional groups could then be hydrolyzed to

hydroxyl groups (Sato, 2008) to form 2-MG and high-MW oligoesters (Route 3 in Fig. 10). However, gas-phase abundances of C_4 - (for methacrolein and crotonaldehyde) or C_5 - (for 2M2B, 3M2B and 2-pentenal) hydroxynitrate-PAN, the supposed SOA intermediate in all these systems, do not correlate with the amount of aerosol formed. Substitution of the α -carbon atom by methyl groups (from crotonaldehyde to methacrolein, or from 3M2B to 2M2B) leads to an increase in the amount of SOA formed by more than a factor of 4, but no increase in gas-phase signal of the hydroxynitrate-PAN is observed (see Fig. 12), implying that it is unlikely the SOA-forming channel.

Another possible mechanism is that in which after OH addition to the double bond in MPAN the OH-adduct undergoes intramolecular rearrangement before addition of O_2 , leading to formation of 2-MG and oligoesters (Route 1 in Fig. 10). Such isomerization can be competitive with O_2 addition, as the O-O bond in the peroxy nitrate moiety is weak. In one experiment (17/12/09), the chambers were flushed with nitrogen to lower the oxygen content to 2%, thereby slowing down addition of O_2 by a factor of 10. Compared to another experiment with 21% O_2 (16/12/09), no increase in aerosol formation is observed, suggesting that SOA formation likely involves O_2 addition to the MPAN-OH adduct, though it is also possible that the intramolecular rearrangement reaction

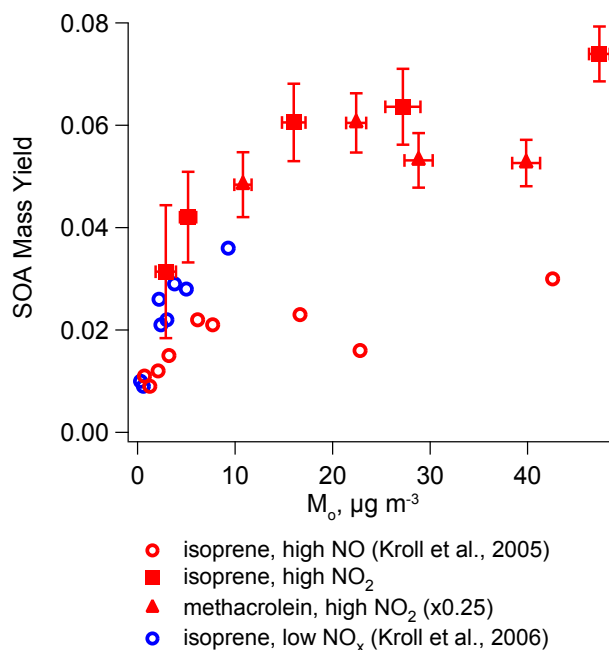


Fig. 11. SOA mass yields from isoprene photooxidation under neutral seed conditions as a function of organic loading. The solid markers indicate SOA yields measured in this study, using CH₃ONO as the OH precursor under high NO₂/NO ratios (between 3 and 8). The SOA yields for methacrolein (solid red triangles) have been multiplied by 0.25 to account for the gas-phase product yield of methacrolein from isoprene high-NO_x oxidation. The SOA yields measured under high-NO₂/NO conditions are higher than both high-NO (open red circles) and low-NO_x conditions (open blue circles) under neutral seed conditions. With an acidified seed, SOA yields can be as high as 0.29 (Surratt et al., 2010).

is sufficiently fast that O₂ addition is not competitive at these O₂ levels.

From the trends of SOA formation observed in the unsaturated aldehyde systems, it appears that the chemical environment of the carbon atom adjacent to the aldehyde group plays an important role in determining the extent of SOA formation. Low-volatility oligoesters are formed only when the α - and β -carbon atoms are unsaturated; SOA yields of 4-pentenal, for which the olefinic bond is in the 4-position, are lower than those of 2-pentenal, and the SOA products are not analogous to those found in SOA from α , β -unsaturated aldehydes (see Fig. 13). SOA formation is correlated with fraction of OH addition to the β -carbon atom, which forms a radical at the α site: SOA yields of crotonaldehyde and 2-pentenal (in which OH addition to the β -carbon is favored) exceed those of 3M2B (in which OH addition to the α -carbon is favored), even though 3M2B has an equal or higher molecular weight. This suggests that an interaction responsible for producing low-volatility species occurs between the peroxy nitrate functional group and the α -carbon (likely a radical species) that our experiments are not able to precisely re-

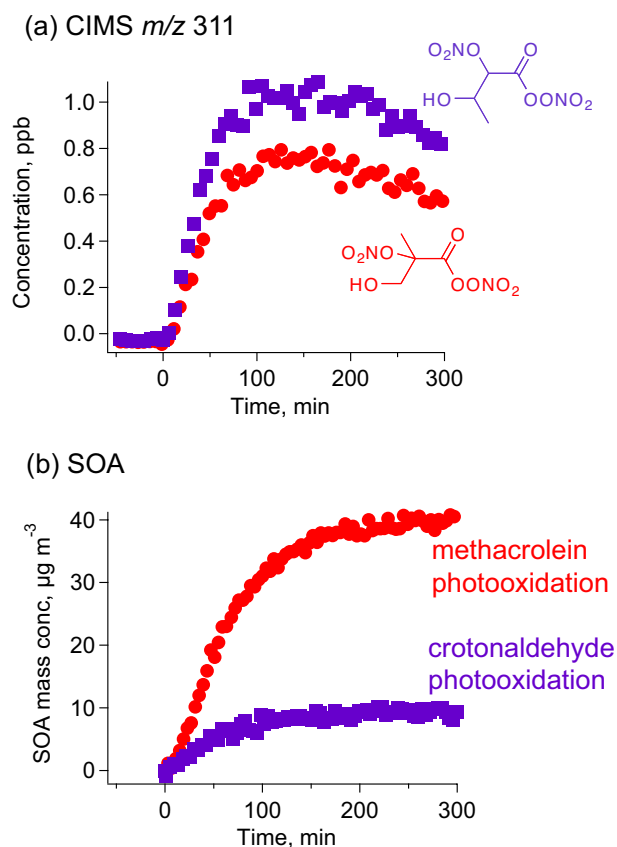


Fig. 12. Time trends of (a) gas-phase CIMS m/z 311 and (b) SOA growth during high-NO₂ photooxidation of methacrolein (red) and crotonaldehyde (purple). m/z 311 corresponds to the unit mass of CF₃O⁻ adduct of C₄-hydroxynitrate-PAN. The observed gas-phase signals of C₄-hydroxynitrate-PAN in both experiments are within 20% of each other, but the amount of SOA formed from methacrolein photooxidation is about a factor of 4 higher. A similar difference was observed between 2M2B and 3M2B photooxidation. This suggests that C₄- and C₅-hydroxynitrate-PANs are not precursors to low-volatility aerosol-phase products.

veal. We hypothesize that the peroxy radical undergoes self cyclization to form a highly reactive dioxoketone intermediate, which subsequently reacts with H₂O or HNO₃ heterogeneously to form the low-volatility products observed in the SOA (see Fig. 10). This intermediate is likely short-lived, and further work is required to identify this species and its role in SOA formation.

One possible explanation for the higher SOA yields observed from methacrolein and 2M2B is that for these compounds SOA formation is favored by steric hindrance. With an additional methyl group on the α carbon, steric repulsion causes the methyl group to move away from the neighbouring peroxy nitrate functional group by rotation of the C-C bond. As a result, the intramolecular reaction leading to SOA formation can be enhanced, consistent with the relatively higher SOA yields. For the other α , β -unsaturated

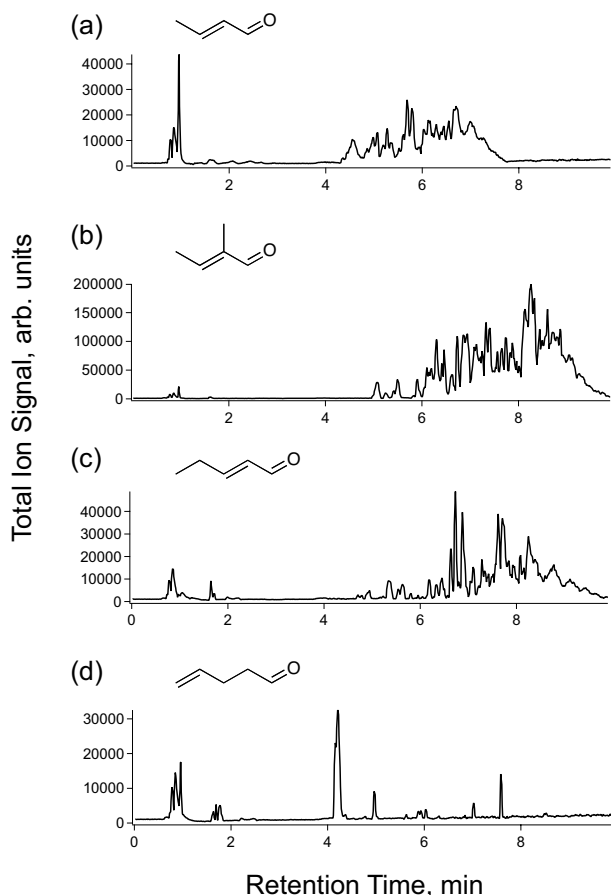
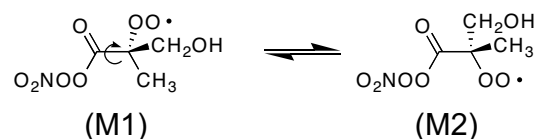


Fig. 13. UPLC/(-)ESI-TOFMS base peak ion chromatograms (BPCs) for high-NO₂ photooxidation of (a) crotonaldehyde (b) 2M2B (c) 2-pentenal and (d) 4-pentenal. The exact masses and elemental composition of detected [M-H]⁻ ions are listed in the Supplementary Material. Compounds detected in crotonaldehyde, 2M2B and 2-pentenal SOA are likely similar. (SOA products from C₅ 2M2B and 2-pentenal are less polar than those from crotonaldehyde, a C₄ compound, and therefore have longer retention times in reverse-phase chromatography.) The chemical composition of 4-pentenal SOA is significantly different from those all 3 other aldehydes, and no oligoester products are detected, suggesting a different SOA formation mechanism.

aldehydes, this interaction is likely not favored, as the hydrogen atom on the α carbon is in plane with the peroxy nitrate group in the most stable rotational conformer (see Fig. 14). The interaction between the peroxy nitrate group and the added functional group is reduced, corresponding to lower SOA formation. Thermodynamic calculations of the relative stabilities of the conformers are required to confirm this hypothesis.

Methacrolein:



Crotonaldehyde:

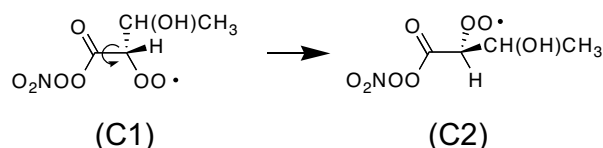


Fig. 14. Rotational conformers of hypothesized SOA intermediate in methacrolein and crotonaldehyde mechanism. For methacrolein, the methyl group on the α -carbon presents significant steric hindrance, which favors the conformer M2. This increases the interaction between the peroxy radical and the peroxy nitrate group, leading to significant SOA formation. For crotonaldehyde, the hydrogen atom presents much smaller steric hindrance, favoring the conformer C2. As a result, the peroxy radical is out of plane with the PAN group, and the reaction to form SOA can be less favorable.

6.2 Methylbutenols (MBO)

MBO232 is a biogenic hydrocarbon potentially important in forest photochemistry (Harley et al., 1998). The SOA yields of MBO232 photooxidation have been shown to be negligible, under both high- and low-NO_x conditions (Carrasco et al., 2007; Chan et al., 2009a). In this study, SOA formation from MBO232 photooxidation is below detection limit, even at high NO₂/NO ratios (which would favor any PAN formation). This is likely linked to the lack of PAN products from MBO232 oxidation. The fate of the alkoxy radical formed from OH-initiated oxidation of MBO232 is shown in Fig. 15. Scission of the C-C bond adjacent to the tertiary carbon is favored, leading to high yields of glycolaldehyde (>0.6). Formation of 2-hydroxymethylpropanal (2-HMPR) following scission of the C-C bond adjacent to the primary carbon is not the favored route, and hence the yields of 2-HMPR are relatively low (<0.4). Furthermore, OH oxidation of 2-HMPR proceeds by OH abstraction of the aldehydic hydrogen, but owing to the neighbouring hydroxyl group, decomposition to acetone and CO is favored over addition of O₂ to form an acyl peroxy radical. Carrasco et al. (2006) found no PAN formation from photooxidation of 2-HMPR, despite high NO₂/NO ratios.

MBO231 photooxidation produces, in contrast, substantial amounts of SOA, at mass yields of 0.008 – 0.042. In MBO231, the hydroxyl group is in the 1-position and is not adjacent to the double bond. Decomposition of the analogous alkoxy radical therefore proceeds by scission of the C-C

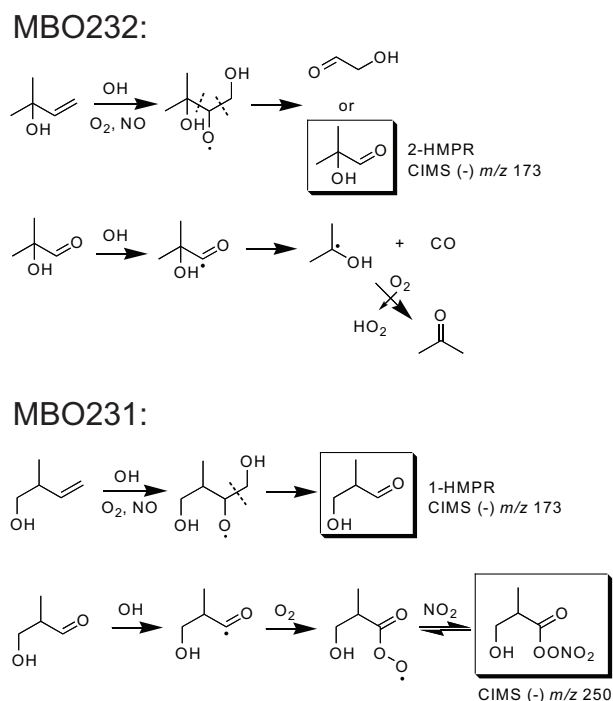


Fig. 15. Mechanism of MBO231 and MBO232 photooxidation under high-NO_x conditions. The dashed lines indicate possible locations of C-C bond scission under decomposition of alkoxy radicals. For MBO232, 2-HMPR formation is relatively small, as scission of the C-C bond with the 4-carbon is not favored. In addition, the acyl radical from H-abstraction of 2-HMPR rapidly decomposes to CO and acetone. As a result, PAN formation is unlikely. For MBO231, 1-HMPR formation is favored from the decomposition of the alkoxy radical. Furthermore, OH reaction of 1-HMPR leads to an acyl peroxy radical, which reacts with NO₂ to form a C₄-hydroxy-PAN.

bond adjacent to the primary carbon, favoring the formation of 1-HMPR; observed HMPR (CIMS (-)*m/z* 173) concentrations in MBO231 photooxidation were twice as high as those in MBO232 photooxidation. Also, following abstraction of the aldehydic hydrogen from 1-HMPR, addition of O₂ to form an acyl peroxy radical is favored over decomposition to CO. Under high-NO₂ conditions, the acyl peroxy radical can react with NO₂ to form a C₄-hydroxy-PAN (see Fig. 15). Tandem mass spectrometry was used to distinguish gas-phase C₄-hydroxy-PAN from the isobaric C₅ dihydroxynitrate, both observed at (-)*m/z* 250 (see Supplementary Material for details). The C₅ dihydroxynitrate is a first generation oxidation product of both MBO231 and MBO232 formed from RO₂+NO at molar yields of 0.10–0.15 (Chan et al., 2009a). In high-NO photooxidation of MBO231 and high-NO₂ photooxidation of MBO232, no C₄-hydroxy-PAN was observed in the gas phase, corresponding to negligible aerosol formation. In high-NO₂ photooxidation of MBO231, C₄-hydroxy-PAN is a major gas-phase product, and SOA formation is significant. The identification of C₄-hydroxy-PAN

is further supported by the ratios of ion signals of *m/z* 250 to *m/z* 251, its ¹³C isotopologue, which indicate that the signal at *m/z* 250 was dominated by a C₄ compound during MBO231 high-NO₂ photooxidation, and by a C₅ compound during MBO232 photooxidation. Hence, the low SOA yields from MBO232 are due to the lack of PAN formation, illustrating the potentially important role of PAN compounds as SOA intermediates.

7 Conclusions

In this work, we systematically investigate the effect of relative NO and NO₂ concentrations on SOA formation from aldehyde photooxidation under high-NO_x conditions. A strong positive correlation of SOA yields with NO₂/NO ratio is observed for methacrolein (a major oxidation product of isoprene responsible for SOA formation) and two related α,β -unsaturated aldehydes, acrolein and crotonaldehyde. Oligoester products from dihydroxycarboxylic acids and hydroxynitrooxycarboxylic acids are also observed to depend on NO₂/NO ratio, confirming that PAN chemistry plays an important role in formation of these low-volatility products. Offline high-resolution aerosol mass spectrometry reveals that analogous oligoester products are major constituents in SOA formed from all α,β -unsaturated aldehydes studied here. By comparing SOA formation from structurally similar aldehydes, we establish that SOA formation is favored when the α -carbon is substituted by a methyl group and the olefinic bond is in the 2-position, such as in methacrolein and 2M2B. The experimental data suggest that SOA formation proceeds via an intramolecular reaction involving the peroxy nitrate functional group, following the addition of O₂ to the MPAN+OH adduct. No aerosol formation is observed from MBO232, an atmospherically important unsaturated alcohol, even at high NO₂/NO ratios, as PAN formation is structurally unfavorable.

Understanding the overall effect of NO_x on SOA yields is important, as SOA yields can vary greatly depending on NO_x conditions. In most photooxidation systems, addition of OH, followed by O₂, to an olefinic bond results in formation of a hydroxyperoxy radical. The competition between the RO₂+HO₂ pathway (which forms low-volatility hydroperoxides) and the RO₂+NO pathway (which forms volatile organic nitrates and fragmentation products) determines the SOA yields. In the isoprene-high-NO_x system, owing to the MPAN chemistry, aerosol formation proceeds via OH abstraction of the aldehydic hydrogen from methacrolein. As a result, a competition exists between reaction of the acyl peroxy radical with NO₂, leading to formation of MPAN and SOA, and with NO to form volatile fragmentation products. The present work shows the importance of the RO₂+NO₂ pathway of unsaturated aldehyde photooxidation as a route leading to SOA formation. This could have important implications on SOA formation from

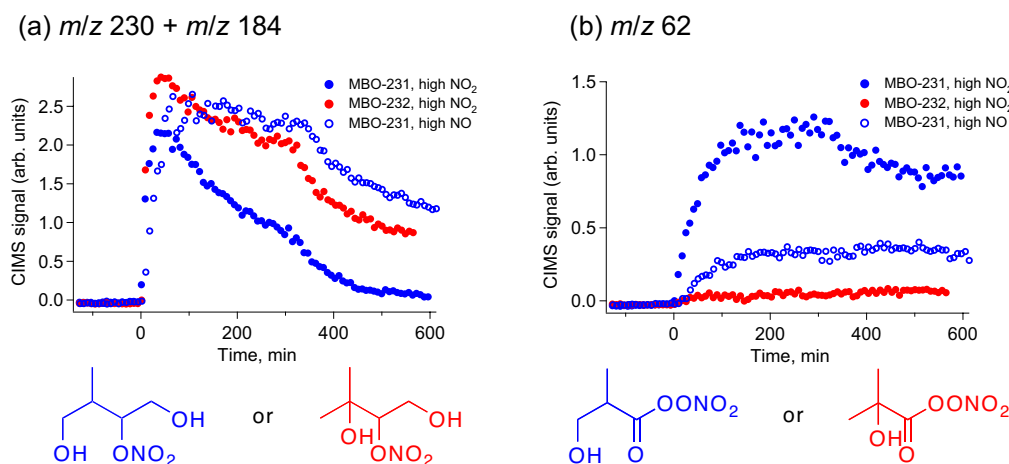


Fig. 16. Gas-phase ion signals of C₄-hydroxy-PAN and C₅-dihydroxynitrate from photooxidation of MBO231 and MBO232, as observed by negative chemical ionization-tandem mass spectrometry of m/z 250. Neutral losses of HF or CF₂O are associated with the C₅-dihydroxynitrate under CID of the parent ion m/z 250, leading to daughter ions of 230 and 184, respectively. The daughter ion m/z 62, most likely NO₃⁻, is associated with the C₄-hydroxy-PAN. (See Supplementary Material for more details.) After 300 minutes of irradiation, more OH precursor was added to further react oxidation products. PAN formation was observed only from MBO231 oxidation and is positively correlated with NO₂/NO, similar to unsaturated aldehydes.

other atmospheric compounds, especially those with conjugated double bonds. For example, photooxidation of aromatic compounds (Calvert et al., 2002) can lead to α , β -unsaturated aldehydes, which can form significant amounts of low-volatility products via a PAN intermediate. At atmospherically relevant NO₂/NO ratios, SOA yields from isoprene are 0.031–0.074 at organic aerosol loadings of 3–47 $\mu\text{g m}^{-3}$; these values are 3 times higher than those previously measured under high-NO conditions. The yields exceed even those measured under low-NO_x conditions. An implication of these results is that atmospheric SOA formation from aldehydes may be significantly underestimated in current models, since an appreciable fraction of SOA is generated in areas where NO₂/NO ratios are high.

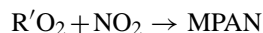
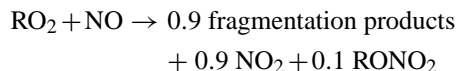
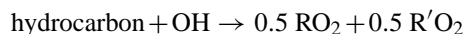
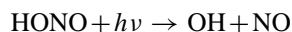
Radiocarbon (¹⁴C) studies have repeatedly shown that ambient organic aerosol is dominated by biogenic carbon, suggesting that biogenic hydrocarbons are an important source of SOA. However, field measurements have shown that organic aerosol levels tend to be correlated with anthropogenic tracers such as CO and acetylene. From satellite observations one can infer that while the source of carbon in many regions is most likely biogenic, the aerosol formation from biogenic hydrocarbons is significantly enhanced by anthropogenic activities (i.e. NO_x and SO_x emissions (Goldstein et al., 2009; Carlton et al., 2010)). The present work moves in the direction of reconciling these two seemingly contradictory observations of biogenic carbon versus anthropogenic enhancement. Here we show that the SOA yields from photooxidation of isoprene under atmospherically relevant NO₂/NO ratios are significantly larger than those previously measured under lower NO₂/NO ratios. Moreover, the SOA yields un-

der these conditions are larger than those under low-NO_x conditions, suggesting that SOA formation from isoprene, the most abundantly emitted non-methane biogenic hydrocarbon, can be more efficient in urban high-NO_x plumes than in remote regions.

Appendix A

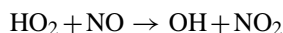
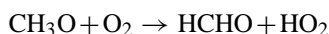
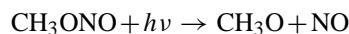
Photochemical modeling to estimate NO and NO₂ concentrations

Owing to interference with the NO₂ signal by HONO and CH₃ONO in the chemiluminescence NO_x monitor, we estimate NO and NO₂ concentrations during chamber experiments by photochemical modeling. In experiments in which HONO is the source of OH, the photolysis rate of HONO is estimated from the first-order decay of the m/z 66 signal on the CIMS, which correspond to the HF·ONO⁻ ion. The initial mixing ratio of HONO was estimated based on the decay of parent hydrocarbon and known rate constants (Atkinson and Arey, 2003; Magneron et al., 2002). Previous comparison to a GC/NO₂ analyzer allows us to determine the HONO interference on the NO₂ signal, and hence the amount of NO and NO₂ produced during HONO synthesis (Chan et al., 2009b). The initial mixing ratio of NO₂ is therefore the sum of the concentrations of NO₂ impurity from HONO synthesis (calculated by multiplying the NO₂ signal after HONO injection by a known factor) and additional NO₂ injected (the increase in NO₂ signal from direct injection). For unsaturated aldehydes, the photochemical model includes the following reactions:



RO₂ denotes the peroxy radical produced by OH addition to the C=C double bond, followed by O₂. R'O₂ denotes the acyl peroxy radical produced by OH abstraction of the aldehydic hydrogen, followed by O₂ addition. These two channels (OH addition and abstraction) have a branching ratio of 1:1 for methacrolein (Tuazon and Atkinson, 1990). Other reactions involving O₃, HO_x, NO_x are also included in the mechanism. For MBO231 and MBO232, the reactions described in Chan et al. (2009a) are used. The calculated NO₂/NO ratios averaged over the first 200 min of irradiation (the period during which SOA formation occurred, see Fig. 1) are listed in Table 2.

For the high-NO₂ experiments, CH₃ONO was used as the OH precursor:



The photolysis rate of CH₃ONO was estimated by the first-order decay of the CH₃ONO signal on GC/FID. The initial mixing ratio of CH₃ONO was determined from the measured vapor pressure of CH₃ONO in the injection bulb. The modeled decay of the hydrocarbon is consistent with that observed by GC/FID. FTIR analysis shows no NO or NO₂ impurities are produced during CH₃ONO synthesis ([NO₂] was less than 0.6% of [CH₃ONO]). In the photochemical calculations, the initial NO and NO₂ concentrations are determined from the increase in NO and NO₂ signals from direct injection. The calculated NO₂/NO ratios averaged over the first 100 min of irradiation are listed in Table 2 (see Fig. 2).

Supplementary material related to this article is available online at:

<http://www.atmos-chem-phys.net/10/7169/2010/acp-10-7169-2010-supplement.pdf>

Acknowledgements. This research was funded by US Department of Energy Biological and Environmental Research Program DE-FG02-05ER63983, US Environmental Protection Agency STAR grant RD-83374901, US National Science Foundation grant ATM-0432377, and the Electric Power Research Institute. This publication has not been formally reviewed by the EPA. The views

expressed in this document are solely those of the authors and EPA does not endorse any products mentioned in this publication. The authors would like to thank K. E. Kautzman and A. J. Kwan for experimental assistance, and F. Paulot for helpful discussion.

Edited by: M. Gysel

References

- Atkinson, R. and Arey, J.: Atmospheric degradation of volatile organic compounds, *Chem. Rev.*, 103, 4605–4638, 2003.
- Calvert, J. G., Atkinson, R., Becker, K. H., Kamens, R. M., Seinfeld, J. H., Wallington, T. J., and Yarwood, G.: The mechanisms of atmospheric oxidation of aromatic hydrocarbons, Oxford University Press, 2002.
- Canagaratna, M. R., Jayne, J. T., Jimenez, J. L., Allan, J. D., Alfarra, M. R., Zhang, Q., Onasch, T. B., Drewnick, F., Coe, H., Middlebrook, A., Delia, A., Williams, L. R., Trimborn, A. M., Northway, M. J., DeCarlo, P. F., Kolb, C. E., Davidovits, P., and Worsnop, D. R.: Chemical and microphysical characterization of ambient aerosols with the Aerodyne aerosol mass spectrometer, *Mass. Spec. Rev.*, 26, 185–222, 2007.
- Carlton, A. G., Wiedinmyer, C., and Kroll, J. H.: A review of Secondary Organic Aerosol (SOA) formation from isoprene, *Atmos. Chem. Phys.*, 9, 4987–5005, doi:10.5194/acp-9-4987-2009, 2009.
- Carlton, A. G., Pinder, R. W., Bhave, P. V. and Pouliot, G. A.: To what extent can biogenic SOA be controlled? *Environ. Sci. Technol.*, 44, 3376–3380, 2010.
- Carrasco, N., Doussin, J. F., Picquet-Varrault, B., and Carlier, P.: Tropospheric degradation of 2-hydroxy-2-methylpropanal, a photo-oxidation product of 2-methyl-3-buten-2-ol: Kinetic and mechanistic study of its photolysis and its reaction with OH radicals, *Atmos. Environ.*, 40, 2011–2019, 2006.
- Carrasco, N., Doussin, J. F., O'Connor, M., Wenger, J. C., Picquet-Varrault, B., Durand-Jolibois, R., and Carlier, P.: Simulation chamber studies of the atmospheric oxidation of 2-methyl-3-buten-2-ol: Reaction with hydroxyl radicals and ozone under a variety of conditions, *J. Atmos. Chem.*, 56, 33–55, 2007.
- Chan, A. W. H., Galloway, M. M., Kwan, A. J., Chhabra, P. S., Keutsch, F. N., Wennberg, P. O., Flagan, R. C., and Seinfeld, J. H.: Photooxidation of 2-methyl-3-buten-2-ol (MBO) as a potential source of secondary organic aerosol, *Environ. Sci. Technol.*, 43, 4647–4652, 2009a.
- Chan, A. W. H., Kautzman, K. E., Chhabra, P. S., Surratt, J. D., Crouse, J. D., Kürten, A., Wennberg, P. O., Flagan, R. C., Seinfeld, J. H.: Secondary organic aerosol formation from photooxidation of naphthalene and alkylnaphthalenes: implications for oxidation of intermediate volatility organic compounds (IVOCs), *Atmos. Chem. Phys.*, 9, 3049–3060, doi:10.5194/acp-9-3049-2009, 2009.
- Chung, S. H. and Seinfeld, J. H.: Global distribution and climate forcing of carbonaceous aerosols, *J. Geophys. Res.-Atmos.*, 107, doi:10.1029/2001JD001397, 2002.
- Claeys, M., Graham, B., Vas, G., Wang, W., Vermeylen, R., Pashynska, V., Cafmeyer, J., Guyon, P., Andreae, M. O., Artaxo, P., and Maenhaut, W.: Formation of secondary organic aerosols through photooxidation of isoprene, *Science*, 303, 1173–1176, 2004.

- Cocker, D. R., Flagan, R. C., and Seinfeld, J. H.: State-of-the-art chamber facility for studying atmospheric aerosol chemistry, *Environ. Sci. Technol.*, 35, 2594–2601, 2001.
- Crouse, J. D., McKinney, K. A., Kwan, A. J., and Wennberg, P. O.: Measurement of gas-phase hydroperoxides by chemical ionization mass spectrometry, *Anal. Chem.*, 78, 6726–6732, 2006.
- de Gouw, J. A., Middlebrook, A. M., Warneke, C., Goldan, P. D., Kuster, W. C., Roberts, J. M., Fehsenfeld, F. C., Worsnop, D. R., Canagaratna, M. R., Pszenny, A. A. P., Keene, W. C., Marchewka, M., Bertman, S. B., and Bates, T. S.: Budget of organic carbon in a polluted atmosphere: Results from the New England Air Quality Study in 2002, *J. Geophys. Res.-Atmos.*, 110, D16305, doi:10.1029/2004JD005623, 2005.
- de Gouw, J. A., Brock, C. A., Atlas, E. L., Bates, T. S., Fehsenfeld, F. C., Goldan, P. D., Holloway, J. S., Kuster, W. C., Lerner, B. M., Matthew, B. M., Middlebrook, A. M., Onasch, T. B., Peltier, R. E., Quinn, P. K., Senff, C. J., Stohl, A., Sullivan, A. P., Trainer, M., Warneke, C., Weber, R. J., and Williams, E. J.: Sources of particulate matter in the northeastern United States in summer: 1. Direct emissions and secondary formation of organic matter in urban plumes, *J. Geophys. Res.-Atmos.*, 113, D08301, doi:10.1029/2007JD009243, 2008.
- DeCarlo, P. F., Kimmel, J. R., Trimborn, A., Northway, M. J., Jayne, J. T., Aiken, A. C., Gonin, M., Fuhrer, K., Horvath, T., Docherty, K. S., Worsnop, D. R., and Jimenez, J. L.: Field-deployable, high-resolution, time-of-flight aerosol mass spectrometer, *Anal. Chem.*, 78, 8281–8289, 2006.
- Dommen, J., Metzger, A., Duplissy, J., Kalberer, M., Alfarra, M. R., Gascho, A., Weingartner, E., Prevot, A. S. H., Verheggen, B., and Baltensperger, U.: Laboratory observation of oligomers in the aerosol from isoprene/NO_x photooxidation, *Geophys. Res. Lett.*, 33, L13805, doi:10.1029/2006GL026523, 2006.
- Edney, E. O., Kleindienst, T. E., Jaoui, M., Lewandowski, M., Offenberger, J. H., Wang, W., and Claeys, M.: Formation of 2-methyl tetrols and 2-methylglyceric acid in secondary organic aerosol from laboratory irradiated isoprene/NO_x/SO₂/air mixtures and their detection in ambient PM_{2.5} samples collected in the eastern United States, *Atmos. Environ.*, 39, 5281–5289, 2005.
- Fantechi, G., Jensen, N. R., Hjorth, J., and Peeters, J.: Determination of the rate constants for the gas-phase reactions of methyl butenol with OH radicals, ozone, NO₃ radicals, and Cl atoms, *Int. J. Chem. Kinet.*, 30, 589–594, 1998.
- Galloway, M. M., Chhabra, P. S., Chan, A. W. H., Surratt, J. D., Flagan, R. C., Seinfeld, J. H., and Keutsch, F. N.: Glyoxal uptake on ammonium sulphate seed aerosol: reaction products and reversibility of uptake under dark and irradiated conditions, *Atmos. Chem. Phys.*, 9, 3331–3345, doi:10.5194/acp-9-3331-2009, 2009.
- Goldstein, A. H., Koven, C. D., Heald, C. L., and Fung, I. Y.: Biogenic carbon and anthropogenic pollutants combine to form a cooling haze over the southeastern United States, *Proc. Natl. Acad. Sci. USA*, 106, 8835–8840, 2009.
- Guenther, A., Karl, T., Harley, P., Wiedinmyer, C., Palmer, P. I., and Geron, C.: Estimates of global terrestrial isoprene emissions using MEGAN (Model of Emissions of Gases and Aerosols from Nature), *Atmos. Chem. Phys.*, 6, 3181–3210, doi:10.5194/acp-6-3181-2006, 2006.
- Hallquist, M., Wenger, J. C., Baltensperger, U., Rudich, Y., Simpson, D., Claeys, M., Dommen, J., Donahue, N. M., George, C., Goldstein, A. H., Hamilton, J. F., Herrmann, H., Hoffmann, T., Iinuma, Y., Jang, M., Jenkin, M. E., Jimenez, J. L., Kiendler-Scharr, A., Maenhaut, W., McFiggans, G., Mentel, Th. F., Monod, A., Prvt, A. S. H., Seinfeld, J. H., Surratt, J. D., Szmigielski, R., and Wildt, J.: The formation, properties and impact of secondary organic aerosol: current and emerging issues, *Atmos. Chem. Phys.*, 9, 5155–5236, doi:10.5194/acp-9-5155-2009, 2009.
- Harley, P., Fridd-Stroud, V., Greenberg, J., Guenther, A., and Vancinello, P.: Emission of 2-methyl-3-buten-2-ol by pines: A potentially large natural source of reactive carbon to the atmosphere, *J. Geophys. Res.-Atmos.*, 103, 25479–25486, 1998.
- Hatakeyama, S., Izumi, K., Fukuyama, T., Akimoto, H., and Washida, N.: Reactions of OH with alpha-pinene and beta-pinene in air – Estimate of global CO production from the atmospheric oxidation of terpenes, *J. Geophys. Res.-Atmos.*, 96, 947–958, 1991.
- Henze, D. K. and Seinfeld, J. H.: Global secondary organic aerosol from isoprene oxidation, *Geophys. Res. Lett.*, 33, L09812, doi:10.1029/2006GL025976, 2006.
- Henze, D. K., Seinfeld, J. H., Ng, N. L., Kroll, J. H., Fu, T.-M., Jacob, D. J., and Heald, C. L.: Global modeling of secondary organic aerosol formation from aromatic hydrocarbons: high- vs. low-yield pathways, *Atmos. Chem. Phys.*, 8, 2405–2420, doi:10.5194/acp-8-2405-2008, 2008.
- Hurley, M. D., Sokolov, O., Wallington, T. J., Takekawa, H., Karasawa, M., Klotz, B., Barnes, I., and Becker, K. H.: Organic aerosol formation during the atmospheric degradation of toluene, *Environ. Sci. Technol.*, 35, 1358–1366, 2001.
- Ion, A. C., Vermeylen, R., Kourtchev, I., Cafmeyer, J., Chi, X., Gelencsr, A., Maenhaut, W., and Claeys, M.: Polar organic compounds in rural PM_{2.5} aerosols from K-puszt, Hungary, during a 2003 summer field campaign: Sources and diel variations, *Atmos. Chem. Phys.*, 5, 1805–1814, doi:10.5194/acp-5-1805-2005, 2005.
- Johnson, D., Jenkin, M. E., Wirtz, K., and Martin-Reviejo, M.: Simulating the formation of secondary organic aerosol from the photooxidation of aromatic hydrocarbons, *Environ. Chem.*, 2, 35–48, 2005.
- Kanakidou, M., Seinfeld, J. H., Pandis, S. N., Barnes, I., Dentener, F. J., Facchini, M. C., Van Dingenen, R., Ervens, B., Nenes, A., Nielsen, C. J., Swietlicki, E., Putaud, J. P., Balkanski, Y., Fuzzi, S., Horth, J., Moortgat, G. K., Winterhalter, R., Myhre, C. E. L., Tsigaridis, K., Vignati, E., Stephanou, E. G., and Wilson, J.: Organic aerosol and global climate modelling: a review, *Atmos. Chem. Phys.*, 5, 1053–1123, doi:10.5194/acp-5-1053-2005, 2005.
- Keyword, M. D., Varutbangkul, V., Bahreini, R., Flagan, R. C., and Seinfeld, J. H.: Secondary organic aerosol formation from the ozonolysis of cycloalkenes and related compounds, *Environ. Sci. Technol.*, 38, 4157–4164, 2004.
- Kleindienst, T. E., Lewandowski, M., Offenberger, J. H., Jaoui, M., and Edney, E. O.: The formation of secondary organic aerosol from the isoprene + OH reaction in the absence of NO_x, *Atmos. Chem. Phys.*, 9, 6541–6558, doi:10.5194/acp-9-6541-2009, 2009.
- Kourtchev, I., Ruuskanen, T., Maenhaut, W., Kulmala, M., and Claeys, M.: Observation of 2-methyltetrols and related photo-oxidation products of isoprene in boreal forest aerosols from

- Hyttiälä, Finland, *Atmos. Chem. Phys.*, 5, 2761–2770, doi:10.5194/acp-5-2761-2005, 2005.
- Kroll, J. H. and Seinfeld, J. H.: Chemistry of secondary organic aerosol: Formation and evolution of low-volatility organics in the atmosphere, *Atmos. Environ.*, 42, 3593–3624, 2008.
- Kroll, J. H., Ng, N. L., Murphy, S. M., Flagan, R. C., and Seinfeld, J. H.: Secondary organic aerosol formation from isoprene photooxidation under high-NO_x conditions, *Geophys. Res. Lett.*, 32, L18808, doi:10.1029/2005GL023637, 2005a.
- Kroll, J. H., Ng, N. L., Murphy, S. M., Varutbangkul, V., Flagan, R. C., and Seinfeld, J. H.: Chamber studies of secondary organic aerosol growth by reactive uptake of simple carbonyl compounds, *J. Geophys. Res.-Atmos.*, 110, D23207, doi:10.1029/2005JD006004, 2005b.
- Kroll, J. H., Ng, N. L., Murphy, S. M., Flagan, R. C., and Seinfeld, J. H.: Secondary organic aerosol formation from isoprene photooxidation, *Environ. Sci. Technol.*, 40, 1869–1877, 2006.
- Lewis, C. W. and Stiles, D. C.: Radiocarbon content of PM_{2.5} ambient aerosol in Tampa, FL, *Aerosol. Sci. Tech.*, 40, 189–196, 2006.
- Lewis, C. W., Klouda, G. A., and Ellenson, W. D.: Radiocarbon measurement of the biogenic contribution to summertime PM_{2.5} ambient aerosol in Nashville, TN, *Atmos. Environ.*, 38, 6053–6061, 2004.
- Liggio, J., Li, S. M., and McLaren, R.: Heterogeneous reactions of glyoxal on particulate matter: Identification of acetals and sulfate esters, *Environ. Sci. Technol.*, 39, 1532–1541, 2005.
- Magneron, I., Thevenet, R., Mellouki, A., Le Bras, G., Moortgat, G. K., and Wirtz, K.: A study of the photolysis and OH-initiated oxidation of acrolein and trans-crotonaldehyde, *J. Phys. Chem. A.*, 106, 2526–2537, 2002.
- Ng, N. L., Chhabra, P. S., Chan, A. W. H., Surratt, J. D., Kroll, J. H., Kwan, A. J., McCabe, D. C., Wennberg, P. O., Sorooshian, A., Murphy, S. M., Dalleska, N. F., Flagan, R. C., and Seinfeld, J. H.: Effect of NO_x level on secondary organic aerosol (SOA) formation from the photooxidation of terpenes, *Atmos. Chem. Phys.*, 7, 5159–5174, doi:10.5194/acp-7-5159-2007, 2007a.
- Ng, N. L., Kroll, J. H., Chan, A. W. H., Chhabra, P. S., Flagan, R. C., and Seinfeld, J. H.: Secondary organic aerosol formation from m-xylene, toluene, and benzene, *Atmos. Chem. Phys.*, 7, 3909–3922, doi:10.5194/acp-7-3909-2007, 2007b.
- Orlando, J. J., Tyndall, G. S., and Paulson, S. E.: Mechanism of the OH-initiated oxidation of methacrolein, *Geophys. Res. Lett.*, 26, 2191–2194, 1999.
- Orlando, J. J., Tyndall, G. S., Bertman, S. B., Chen, W. C., and Burkholder, J. B.: Rate coefficient for the reaction of OH with CH₂=C(CH₃)C(O)OONO₂ (MPAN), *Atmos. Environ.*, 36, 1895–1900, 2002.
- Pandis, S. N., Paulson, S. E., Seinfeld, J. H., and Flagan, R. C.: Aerosol formation in the photooxidation of isoprene and beta-pinene, *Atmos. Environ.*, 25, 997–1008, 1991.
- Paulot, F., Crounse, J. D., Kjaergaard, H. G., Kurten, A., St Clair, J. M., Seinfeld, J. H., and Wennberg, P. O.: Unexpected epoxide formation in the gas-phase photooxidation of isoprene, *Science*, 325, 730–733, 2009.
- Presto, A. A., Hartz, K. E. H., and Donahue, N. M.: Secondary organic aerosol production from terpene ozonolysis. 2. Effect of NO_x concentration, *Environ. Sci. Technol.*, 39, 7046–7054, 2005.
- Sato, K.: Detection of nitrooxypolyols in secondary organic aerosol formed from the photooxidation of conjugated dienes under high-NO_x conditions, *Atmos. Environ.*, 42, 6851–6861, 2008.
- Song, C., Na, K. S., and Cocker, D. R.: Impact of the hydrocarbon to NO_x ratio on secondary organic aerosol formation, *Environ. Sci. Technol.*, 39, 3143–3149, 2005.
- Surratt, J. D., Murphy, S. M., Kroll, J. H., Ng, N. L., Hildebrandt, L., Sorooshian, A., Szmigielski, R., Vermeylen, R., Maenhaut, W., Claeys, M., Flagan, R. C., and Seinfeld, J. H.: Chemical composition of secondary organic aerosol formed from the photooxidation of isoprene, *J. Phys. Chem. A*, 110, 9665–9690, 2006.
- Surratt, J. D., Gomez-Gonzalez, Y., Chan, A. W. H., Vermeylen, R., Shahgholi, M., Kleindienst, T. E., Edney, E. O., Offenberg, J. H., Lewandowski, M., Jaoui, M., Maenhaut, W., Claeys, M., Flagan, R. C., and Seinfeld, J. H.: Organosulfate formation in biogenic secondary organic aerosol, *J. Phys. Chem. A*, 112, 8345–8378, 2008.
- Surratt, J. D., Chan, A. W. H., Eddingsaas, N. C., Chan, M. N., Loza, C. L., Kwan, A. J., Hersey, S. P., Flagan, R. C., Wennberg, P. O., and Seinfeld, J. H.: Reactive intermediates revealed in secondary organic aerosol formation from isoprene, *Proc. Natl. Acad. Sci. USA*, 107, 6640–6645, 2010.
- Szmigielski, R., Surratt, J. D., Vermeylen, R., Szmigielska, K., Kroll, J. H., Ng, N. L., Murphy, S. M., Sorooshian, A., Seinfeld, J. H., and Claeys, M.: Characterization of 2-methylglyceric acid oligomers in secondary organic aerosol formed from the photooxidation of isoprene using trimethylsilylation and gas chromatography/ion trap mass spectrometry, *J. Mass. Spectrom.*, 42, 101–116, 2007.
- Taylor, W. D., Allston, T. D., Moscato, M. J., Fazekas, G. B., Kozlowski, R., and Takacs, G. A.: Atmospheric photo-dissociation lifetimes for nitromethane, methyl nitrite, and methyl nitrate, *Int. J. Chem. Kinet.*, 12, 231–240, 1980.
- Tuazon, E. C. and Atkinson, R.: A product study of the gas-phase reaction of methacrolein with the OH radical in the presence of NO_x, *Int. J. Chem. Kinet.*, 22, 591–602, 1990.
- Tuazon, E. C., Aschmann, S. M., Nishino, N., Arey, J., and Atkinson, R.: Kinetics and products of the OH radical-initiated reaction of 3-methyl-2-butenal, *Phys. Chem. Chem. Phys.*, 7, 2298–2304, 2005.
- Volkamer, R., Ziemann, P. J., and Molina, M. J.: Secondary Organic Aerosol Formation from Acetylene (C₂H₂): seed effect on SOA yields due to organic photochemistry in the aerosol aqueous phase, *Atmos. Chem. Phys.*, 9, 1907–1928, doi:10.5194/acp-9-1907-2009, 2009.
- Weber, R. J., Sullivan, A. P., Peltier, R. E., Russell, A., Yan, B., Zheng, M., de Gouw, J., Warneke, C., Brock, C., Holloway, J. S., Atlas, E. L., and Edgerton, E.: A study of secondary organic aerosol formation in the anthropogenic-influenced southeastern United States, *J. Geophys. Res.-Atmos.*, 112, D13302, doi:10.1029/2007JD008408, 2007.
- Zhang, Q., Jimenez, J. L., Canagaratna, M. R., Allan, J. D., Coe, H., Ulbrich, I., Alfarra, M. R., Takami, A., Middlebrook, A. M., Sun, Y. L., Dzepina, K., Dunlea, E., Docherty, K., DeCarlo, P. F., Salcedo, D., Onasch, T., Jayne, J. T., Miyoshi, T., Shimojo, A., Hatakeyama, S., Takegawa, N., Kondo, Y., Schneider, J., Drewnick, F., Borrmann, S., Weimer, S., Demerjian, K., Williams, P., Bower, K., Bahreini, R., Cottrell, L., Griffin,

R. J., Rautiainen, J., Sun, J. Y., Zhang, Y. M., and Worsnop, D. R.: Ubiquity and dominance of oxygenated species in organic aerosols in anthropogenically-influenced Northern Hemisphere midlatitudes, *Geophys. Res. Lett.*, 34, L13801, doi:10.1029/2007GL029979, 2007a.

Zhang, Y., Huang, J. P., Henze, D. K., and Seinfeld, J. H.: Role of isoprene in secondary organic aerosol formation on a regional scale, *J. Geophys. Res.-Atmos.*, 112, D20207, doi:10.1029/2007JD008675, 2007b.